

Repository of the Max Delbrück Center for Molecular Medicine (MDC)  
Berlin (Germany)  
<http://edoc.mdc-berlin.de/14386/>

## Efficacy of CAR T-cell therapy in large tumors relies upon stromal targeting by IFN $\gamma$

---

*Textor, A., Listopad, J.J., Wuehrmann, L.L., Perez, C., Kruschinski, A., Chmielewski, M., Abken, H., Blankenstein, T., Charo, J.*

This is the author's manuscript that had been peer reviewed and was accepted for publication. The final edited form was published in:

Cancer Research. 2014 Dec 1, Volume 74(23): 6796-6805 | doi: 10.1158/0008-5472.CAN-14-0079  
American Association for Cancer Research ►

# **Efficacy of CAR T cell therapy in large tumors relies upon stromal targeting by IFN $\gamma$**

Ana Textor<sup>1</sup>, Joanna J. Listopad<sup>1</sup>, Lara Le Wührmann<sup>1</sup>, Cynthia Perez<sup>1†</sup>, Anna Kruschinski<sup>1</sup>, Markus Chmielewski<sup>2</sup>, Hinrich Abken<sup>2</sup>, Thomas Blankenstein<sup>1,3</sup>, and Jehad Charo<sup>1†</sup>

## **Authors' Affiliations**

<sup>1</sup>Max-Delbrück-Center for Molecular Medicine, 13092 Berlin, Germany

<sup>2</sup>Department I of Internal Medicine, Tumor Genetics, and Center for Molecular Medicine Cologne, University of Cologne, 50931 Cologne, Germany

<sup>3</sup>Institute of Immunology, Charite Campus Buch, 13092 Berlin, Germany

† Present address: Oncology Research Institute, Loyola University Chicago, Maywood IL 60153, Chicago, USA

## **Running Title**

Chimeric Antigen Receptors Reject Solid Tumors

## **Corresponding Author**

Jehad Charo, Oncology Research Institute, Loyola University Chicago, Cardinal Bernardin Cancer Center, 216 S. First Avenue, Room 304, Maywood, IL 60153, Tel. (708) 327-3325, Fax. (708) 327-3158, e-mail: [jecharo@lumc.edu](mailto:jecharo@lumc.edu)

## **Disclosure of Potential Conflicts of Interest**

The authors have no conflicting financial interests.

**Keywords:** Chimeric Antigen Receptor, Solid tumor, Adoptive T cell Therapy, IFN $\gamma$

## **Abstract**

Adoptive T cell therapy using chimeric antigen receptor-modified T cells (CAR-T therapy) has shown dramatic efficacy in patients with circulating lymphoma. However, eradication of solid tumors with CAR-T therapy has not been reported yet to be efficacious. In solid tumors, stroma destruction, due to MHC-restricted cross-presentation of tumor antigens to T cells, may be essential. However, CAR-Ts recognize antigens in an MHC-independent manner on cancer cells but not stroma cells. In this report, we show how CAR-Ts can be engineered to eradicate large established tumors with provision of a suitable CD28 costimulatory signal. In a HER-2-dependent tumor model, tumor rejection by HER-2-specific CAR-Ts was associated with sustained influx and proliferation of the adoptively transferred T cells. Interestingly, tumor rejection did not involve NK cells, but was associated instead with a marked increase in the level of M1 macrophages and a requirement for IFN $\gamma$  receptor expression on tumor stroma cells. Our results argue that CAR-T therapy is capable of eradicating solid tumors through a combination of antigen-independent stroma destruction and antigen-specific tumor cell targeting.

### **Precis**

This preclinical study shows how the inability of engineered T cell therapies to eradicate solid tumors can be overcome by enabling antigen-independent stroma destruction along with antigen-specific tumor cell targeting, providing possible insights into how to dramatically expand the use of these therapies beyond circulating blood tumors where they are currently useful.

## Introduction

T cells can be redirected with new antigen specificity and used for adoptive T cell therapy (ATT) by introducing either a T cell receptor (TCR), or chimeric antigen receptor (CARs). The CAR consists of an antigen (Ag)-binding single chain variable fragment (scFv) antibody domain and a signaling domain, most often the CD3 $\zeta$  endodomain (1). While T cells with CARs (CAR-Ts) containing CD3 $\zeta$  had a moderate anti-tumor effect and poor persistence *in vivo* (2), addition of costimulatory signals as provided by dual signaling domains (e.g. CD28-CD3 $\zeta$ ) has improved the therapeutic effects of CAR-Ts in experimental models (3) and in clinical trials targeting CD19 on B cell malignancies (4,5).

Tumor transplantation models can be of clinical relevance if large established tumors grown for at least two weeks are treated (6). Such solid tumors are difficult to reject, but can be successfully eradicated if the target antigen is recognized through the TCR (7-11). On the other hand, CAR-mediated recognition leads to regression but not complete eradication (3). This could be due to the sub-optimal affinity of the CAR to the target antigen or the different mode of antigen recognition of CARs versus TCRs. In contrast to TCRs, which recognize peptide antigen presented by MHC class I (MHC I), CARs recognize the cognate cell surface antigen by an antibody domain independently of the MHC I. This can be an advantage since tumors escape TCR-mediated ATT by MHC I down-regulation (12), but it can also be a disadvantage because tumor stroma cells cross-presenting surrogate tumor antigen on MHC I needs to be recognized by T cells in order to prevent tumor escape (7). However, it appears that direct recognition of the tumor stroma is less important for tumor rejection if cancer-driving antigens (CDAs) are targeted by TCR-mediated ATT (10,11). CDAs are arguably the best targets because cancer cell proliferation/survival often depends on its continuous expression, as is the case for the human cell line SKOV3 and HER-2 (epidermal growth factor receptor-2) (13), which is termed oncogene addiction (14). HER-2 is normally an overexpressed self-antigen, but in

this study we utilized a mouse model where human HER-2 was expressed only on the SKOV3 tumor cells and not on mouse cells, which makes it a relevant model for tumor-specific antigens targetable by CAR-Ts (e.g. mutant epidermal growth factor receptor (EGFRvIII) or the chaperon Cosmc) (15,16).

Previous studies employing CARs for treatment of xenografted solid human tumors used polyclonal human T cells as recipient cells for the CAR (3,17), a model containing several confounding factors (Supplementary Fig. S1). Human CAR-Ts were allogeneic with regard to the tumor and xenogeneic with regard to the host. In this setting, it is difficult to exclude allo-MHC T cell responses (through the TCR) contributing to therapy effects. Conversely, lack of overt graft-versus-host reactions to the xenogeneic mouse tissues indicates that human T cells perform poorly in mice. An unknown number of species-specific factors necessary for survival and proliferation may impair the function of human T cells in mice. For example, IFN $\gamma$  function is species-specific (18), so that human T cell-derived IFN $\gamma$  cannot act on mouse tumor stroma cells, which had been shown in syngeneic models to be critical in order to prevent tumor recurrence (8,11). To avoid confounding factors with polyclonal human T cells in mice and better dissect the mechanism of tumor eradication by CAR-Ts, we used mouse monoclonal CD8<sup>+</sup> T cells with tumor-unrelated specificity as CAR recipients (OVA-specific OT-1 cells derived from Rag<sup>-/-</sup> mice). This ensured that the CAR-Ts could act only through their CAR but not TCR, that IFN $\gamma$  could act on the tumor stroma but not the human cancer cells and also excluded a potential contribution of CD4<sup>+</sup> T cells on the therapeutic outcome (Supplementary Fig. S1). Here, we first established that eradication of large established tumors can be achieved by HER-2-specific CAR-Ts if provided with costimulatory CD28 signaling (28- $\zeta$ -CAR) (19). This rejection was associated with sustained accumulation, proliferation and differentiation of CAR-Ts to effector memory (TEM) cell type at the tumor site. We finally demonstrated that tumor

rejection by CAR-Ts involved destruction of tumor stroma through IFN $\gamma$ R, independently of NK cell contribution.

## **Materials and Methods**

### **Mice**

All mouse studies were in accordance with institutional, state, and federal (Landesamt für Arbeitsschutz, Gesundheitsschutz und technische Sicherheit, Berlin) guidelines. Albino Rag1<sup>-/-</sup> or Rag2<sup>-/-</sup> (Rag<sup>-/-</sup>) mice, OT-1/Rag1<sup>-/-</sup> and ChRLuc/OT-1/Rag1<sup>-/-</sup> mice were recently described (9). IFN $\gamma$ R<sup>-/-</sup> and Fas<sup>-/-</sup> mice were obtained from Jackson Laboratory (003288 and 000482, respectively) and bred at the MDC animal facility to Rag1<sup>-/-</sup> mice to obtain IFN $\gamma$ R<sup>-/-</sup>/Rag1<sup>-/-</sup> and Fas<sup>-/-</sup>/Rag1<sup>-/-</sup> mice.

### **Retroviral vectors and cells**

HER-2 specific  $\zeta$ -CARs constructs with scFv of different affinities and the 9-28- $\zeta$ -CAR of the intermediate affinity (20) were introduced into the MSCV expression plasmid as earlier described (21). pMSCV vector encoding for GFP (pMIG) was used as mock control. Retroviral supernatants were generated by cotransfecting HEK-T cells with different MSCV-CAR constructs and gag, pol and env encoding pCL-eco vector (Imgenex) as described previously (21). Virus supernatants were collected 48 and 72h post transfection and used for transducing T cells. Human ovarian carcinoma cell line SKOV3 expressing CBG luciferase was described earlier (21). It was authenticated by flow cytometry as described below.

### **Expansion of T cells and retroviral transduction**

Spleens were isolated from OT-1/Rag1<sup>-/-</sup> or ChRLuc/OT-1/Rag1<sup>-/-</sup> mice and prepared as a single cell suspension with 0.8% NH<sub>4</sub>Cl mediated lysis of red blood cells. 1-2x10<sup>6</sup> cells were cultured in 24 well plates in 1 ml of complemented RPMI media (10% FCS, PAN Biotech; 50  $\mu$ g/ml gentamicin, Gibco; and 50  $\mu$ M mercaptoethanol, Gibco)

supplemented with 1 µg/ml anti (α)-CD3, 0.1 µg/ml α-CD28 antibody (Ab) (BD Bioscience) and 10 IU/ml IL-2 (Proleukin, Prometheus Laboratories) for 24h at 37°C in 5% CO<sub>2</sub> humidified incubator. Virus supernatants of different CAR constructs and mock control produced by HEK-T cells were collected, filtered (0.45 µm pore size) and either used directly for transduction or stored at -80°C. After 24h activation, media was removed from the splenocytes and replaced with 1 ml/well virus supernatant containing 10 µg/ml polybrene (Sigma-Aldrich). The cells were spinoculated for 2h at 800xg and 32°C. Virus supernatant was removed and replaced with 1 ml RPMI containing 10 IU IL-2. Cells were transduced twice, with an interval of 24h. The level of surface CAR expression was measured 24 or 48h after the last transduction.

### **Flow cytometry**

Surface expression of the CARs was measured by staining with the F(ab)<sub>2</sub> fragment from goat anti-human Ig polyclonal Ab conjugated to PE, APC or Dylight 649 (Southern Biotech or Jackson). Additionally cells were stained with α-CD8-APC (or FITC) (clone 53-6.7, BD Bioscience) and α-CD3-FITC Ab (clone G4.18, BD Bioscience). CAR-Ts were also analyzed for activation markers using α-CD44-FITC (clone IM7, BD Bioscience) and α-CD62L-PE (clone MEL-14, BD Bioscience), and for proliferation markers by α-KI-67 (Alexa Flour 488 clone B56, BD Bioscience) and Propidium Iodide staining Solution (BD Bioscience). NK cells were analyzed using α-NK1.1-APC (clone PK136, Biolegend) and α-CD49b-PE (pan-NK-cells, clone DX5, Biolegend) Ab. Macrophages were identified using α-F480-BV421 (clone BM8, Biolegend), α-CD11b-PE (clone M1/70, Biolegend) and additionally stained with α-IA-IE-PeCy7 (clone M5/114.15.2, Biolegend). Tumor samples were additionally analyzed by α-CD45.2-APC (clone 104, Biolegend) and α-Her2neu-PE (clone Neu 24.7, BD Bioscience) Ab. SKOV3 cells were stained with α-Her2neu-PE and with α-HLA-ABC (clone G46-2.6, BD Bioscience) as described earlier to confirm the species

origin and HER-2 expression (21). Data acquisition was performed on a FACS Calibur (BD Biosciences), MACSquant (Miltenyi Biotec) or FACSCanto (BD Biosciences), and the analysis was done by FlowJo (Tree Star) software.

### **Tumor digestion and cytokine release assay**

A third or a half of the isolated tumor was sliced into small pieces and incubated for 1 hour at 37°C in 10 ml digestion solution (complete RPMI medium with collagenase II (1 mg/ml, Gibco), Dispase II (1 mg/ml, Roche) and DNase I (10 µg/ml, Roche). Tumor cells were passed through a cell strainer (40 µm), washed with PBS and treated with ACK lysis buffer. Counted cells were prepared for flow cytometry analysis by incubation with α-FC receptor Ab (TruStain fcX, Biolegend) for 15 min at 4°C. CD8 T cells were purified from tumor cells by using α-CD8a (Ly-2) Microbeads (Miltenyi Biotec) according to the manufacturer's protocol.

To measure cytokine release, CAR-Ts were mixed with mock transduced T cells to equalize the CAR<sup>+</sup> cells between the different constructs in total of  $2 \times 10^5$  cells per construct, from which  $1 \times 10^4$  were CAR<sup>+</sup>. The CAR-Ts were then cocultured with titrated numbers of target SKOV3 tumor cells in 96-well flat bottom plates and 24-48h later IFN $\gamma$  and IL-2 levels were measured in the supernatants by ELISA (BD Biosciences) according to the manufacturer's protocol.

### **Tumor challenge and adoptive T cell transfer**

Age and sex matched mice were injected with  $5 \times 10^6$  SKOV3-CBG tumor cells subcutaneously. On the day of treatment mice received i.v. injection of (unless otherwise indicated)  $2 \times 10^6$  CAR-Ts or mock T cells, resuspended in 100 µl PBS. Tumor size was measured by an electronic caliper and the average tumor diameter was calculated from the measurements of length, width and the depth of the tumor (9). Mice were sacrificed when the tumors reached 15 mm in any one dimension. To confirm the complete tumor rejection, at the end of the treatment experiments (at least 60 days after no palpable tumor was detected), tumor free mice were imaged

for CBG luciferase signal emitted by any potentially remaining SKOV3 cells as described (21). NK cell depletion was achieved by weekly i.p. injection of 160  $\mu\text{g}/\text{mouse}$  of  $\alpha\text{-NK1.1}$  Ab (clone PK136, BioXCell) or isotype control (IgG2a, BioXCell) throughout the experiment. NK cell depletion was confirmed several times over the time-course of the experiment. Tumor free mice from this experiment were observed for at least one week following tumor rejection and the rejection was confirmed by BLI.

### **Bioluminescence imaging**

*In vivo* imaging was performed using a Xenogen IVIS 200 (Caliper Lifescience). A maximum of five anaesthetized mice were imaged at once. Each mouse received an i.v. injection of freshly prepared coelenterazine (Biosynth) that was dissolved in DMSO (Sigma) and diluted in PBS (100  $\mu\text{g}/100 \mu\text{l}$  per mouse) as earlier described (9). Images were acquired for 1 min using small binning, unless saturated signal was obtained, in which case the acquisition was repeated using 10s imaging time. All data were analyzed using Living Image analysis software (Caliper Lifescience). The region of interest (ROI) for the measured signal was drawn at the tumor site identically for all mice and was set anew for each experiment.

## **Results**

### **Increasing the affinity of a $\zeta$ -CAR does not improve the T cell function**

HER-2 specific CARs were cloned into the pMSCV retroviral vector resulting in five CARs with CD3 $\zeta$  signaling domain ( $\zeta$ -CARs) with the affinities of their scFv's between  $10^{-7}$  and  $10^{-11}$  M (Figure 1A), and one CAR with CD3 $\zeta$  and CD28 signaling domains (28- $\zeta$ -CAR) with the affinity of  $10^{-9}$  M (Figure 1A). Following retroviral transduction of mouse splenocytes, the percentage of CAR<sup>+</sup> CD8<sup>+</sup> T cells was generally lower for the  $\zeta$ -CARs (8.5%; SD  $\pm$  5%) when compared to the 9-28- $\zeta$ -CAR (18.5%; SD  $\pm$  13%)

(Figure 1B and Supplementary Fig. S2). Human T cells targeted with these same  $\zeta$ -CARs responded at a very similar level above the affinity threshold of  $1.6 \times 10^{-8}$  M (20). Similarly, 8- $\zeta$ -CAR-Ts responded by secreting more IFN $\gamma$  compared to 7- $\zeta$ -CAR-Ts and levels of IFN $\gamma$  did not increase with CARs of higher affinity, including the 9-28- $\zeta$ -CAR (Figure 1C). CAR-Ts can secrete IL-2 when stimulated through their endogenous CD28 receptor (22) or the chimeric CD28- $\zeta$  receptor (19). Accordingly, we found that CAR-Ts engineered with 9-28- $\zeta$  but not  $\zeta$ -CARs secreted IL-2 (Figure 1C).

We next investigated the ability of  $\zeta$ -CAR-Ts to reject SKOV3 tumors *in vivo* and whether an increase in scFv affinity influences therapeutic outcome. Rag<sup>-/-</sup> mice were subcutaneously (s.c.) injected with  $5 \times 10^6$  SKOV3 cells. About 3 weeks later when the tumors were 6.6 mm (SD  $\pm$  1.1 mm) in average diameter, the mice were treated intravenously (i.v.) with  $2 \times 10^6$  CAR-Ts transduced with mock (GFP) retrovirus or the different affinity  $\zeta$ -CARs. Tumors in mice that received 7- $\zeta$ -CAR-Ts progressed unimpaired comparable to mock-treated mice (Figure 2 and Table 1). Similarly,  $\zeta$ -CAR-Ts of the other affinities (including the highest affinity 11- $\zeta$ -CAR) did not reject SKOV3 tumors and, if at all, only slightly delayed tumor progression (Figure 2 and Table 1).

### **Costimulation by the 28- $\zeta$ -CAR leads to rejection of large established tumors**

To determine if addition of an costimulatory CD28 signaling to the CAR molecule would lead to rejection of SKOV3 tumors, tumor-bearing mice were treated with CAR-Ts expressing either 9- $\zeta$ - or 9-28- $\zeta$ -CAR, which contain the same scFv domain (KD:  $1 \times 10^{-9}$  M) but different signaling domains. As before, tumors grown for ~3 weeks (average tumor diameter 7.1 mm, SD  $\pm$  0.4 mm) progressed in mice receiving 9- $\zeta$ -CAR-Ts or mock treatment, but were long-term rejected by 9-28- $\zeta$ -CAR-Ts (mice remained tumor free 60 days post rejection) (Figure 3A and Table 1). Although both groups received  $2 \times 10^6$  transduced CD8<sup>+</sup> T cells, due to the different transduction

efficiency, 9-28- $\zeta$ -CAR-Ts treated mice received more CAR-Ts ( $5.6 \times 10^5$ ) than 9- $\zeta$ -CAR-Ts treated mice ( $1.4 \times 10^5$ ). To account for that and exclude that the different therapeutic outcome was due to transferring different numbers of CAR-Ts, tumor-bearing mice were treated with titrated numbers of 9-28- $\zeta$ -CAR-Ts. Either  $2 \times 10^5$  or  $5 \times 10^4$  CD8<sup>+</sup> T cells were transferred, which equals to  $5.6 \times 10^4$  or  $1.4 \times 10^4$  CAR<sup>+</sup> T cells, respectively. In both cases, tumors were again long-term rejected (Figure 3B and Table 1). To further confirm these results, mice with large established tumors (average tumor diameter 10.5 mm, SD  $\pm$  1.8 mm) received the same number of CAR<sup>+</sup> T cells; either mock treated or injected with  $2 \times 10^6$  CAR-Ts with similar percentage of 9-28- $\zeta$ - or 9- $\zeta$ -CAR<sup>+</sup> cells (8% and 10%, respectively). Once again, 9-28- $\zeta$ -CAR-Ts rejected the tumors (n=2), while tumors in mock-treated and 9- $\zeta$ -CAR-Ts treated mice progressed (Figure 3C and Table 1).

#### **CAR-Ts require costimulation to accumulate at the tumor site and persist *in vivo***

To visualize the *in vivo* dynamics of the CAR-Ts associated with tumor rejection compared to CAR-Ts associated with failed therapy, we introduced CARs into T cells derived from renilla luciferase transgenic mice (ChRLuc/OT-1/Rag<sup>-/-</sup>) (9) and imaged tumor-bearing mice by bioluminescent *in vivo* imaging (BLI) at various time points following T cell transfer. The BLI background signal was set at  $1 \times 10^5$  p/s/cm<sup>2</sup>/sr, which is the highest signal emitted at the tumor site by mock-treated mice, probably reflecting the homeostatic expansion of transferred T cells (Figure 4A). Similar to TCR-mediated tumor rejection (9), the presence and persistence of the CAR-T signal was associated with tumor regression as only 9-28- $\zeta$ -CAR-Ts accumulated at the tumor site (Figure 4A and B). Typically the signal appeared and reached its peak during the second week post ATT (Figure 4B), where it persisted for 2-3 weeks and then gradually declined (Figure 4A and B). The signal from the *in vivo* imaging of 9-28- $\zeta$  CAR transduced T cells indicate that this population contracted in a fast kinetic following 3 cycles of expansion. This is similar to what we have earlier observed

during the rejection of large established tumors by adoptively transferred TCR transgenic T cells (9). It is likely that, following the expansion, the T cells contracted due to the consumption of the limited amount of the homeostatic cytokines required for T cells persistence. In line with this, a similar pattern has been shown in a study with repeated T cells expansion and contraction during the treatment of 1-week-old B16 melanoma by adoptive T cell therapy (23). Interestingly, in that study, this pattern was replaced by a continuous T cell expansion and persistence pattern when the mice also received IL-15 precomplexed with soluble IL-15 receptor  $\alpha$  and IL-21. The last and most substantial contraction phase coincided with tumor rejection. This indicates that during successful adoptive T cell therapy a new cycle of T cell expansion is repeatedly initiated as long as the cognate antigen is available.

Since the SKOV3 cells used in this study were transduced with a click beetle luciferase (CBG) expressing retrovirus (21), we confirmed complete tumor rejection by showing that no remaining tumor cells could be detected by BLI (Figure 4C). The values for the  $\zeta$ -CAR-T imaged-signals did not vary much between the different treatment groups and only a slight increase over background was observed during the BLI time period of 50 days (Figure 4A). By calculating the maximal T cell signal from mock as compared to 9-28- $\zeta$ -CAR-T treated mice (9), we estimated that homeostatic expansion contributed to about 5% of Ag-driven proliferation. Decreasing the lower scale to  $2 \times 10^4$  p/s/cm<sup>2</sup>/sr to visualize the homeostatic expansion of the transferred T cells showed that the signal of  $\zeta$ -CAR-Ts was similar to control treated mice, suggesting these cells were largely ignorant, which was in contrast to the large signal increase of 9-28- $\zeta$ -CAR-Ts treated mice (Supplementary Fig. S3).

**Costimulation by the 28- $\zeta$ -CAR leads to T cell differentiation and proliferation at the tumor site**

Using BLI, we observed that 9-28- $\zeta$ -CAR-Ts expanded in the tumor-bearing mouse and accumulated preferentially at the tumor site (Supplementary Fig. S4). Although BLI allowed us to visualize this accumulation, we could not address the question of whether these cells were also able to proliferate inside the tumor or to evaluate their differentiation status. Since retroviral transduction required antigen-independent T cell activation, 9- $\zeta$ -CAR-, 9-28- $\zeta$ -CAR- and mock-transduced CAR-Ts contained similar numbers of similarly activated T cells. This was confirmed by the high (hi) expression of CD44 and CD62L (CD44<sup>hi</sup>, CD62L<sup>hi</sup>, Figure 5A), which is typical for memory phenotype. Nevertheless, additional *in vivo* activation by costimulation was required as only 9-28- $\zeta$ -CAR-Ts rejected the tumors while 9- $\zeta$ -CAR-Ts did not. Since TCR-mediated tumor rejection favors TEM phenotype (24), we analyzed whether CAR-mediated tumor rejection involved 28- $\zeta$ -CAR-Ts differentiation into TEMs. Approximately four weeks post tumor challenge, mice received  $2 \times 10^5$  CAR<sup>+</sup> cells from total  $1 \times 10^6$  CAR-Ts per mouse (numbers were equalized for all treatments by adding mock cells to CAR transduced T cells). The percentage of CAR<sup>+</sup> T cells following transduction was 20% for 9- $\zeta$ -CAR-Ts and 40% for 9-28- $\zeta$ -CAR-Ts. Similar to the earlier experiments, mice treated with 9-28- $\zeta$ -CAR-Ts but not those treated with 9- $\zeta$ -CAR-Ts rejected the tumor. By analyzing the tumor infiltrating lymphocytes (TILs) we found that the majority of these cells from the mock- and the 9- $\zeta$ -CAR-Ts-treated mice of the CD8<sup>+</sup>/CD44<sup>+</sup> population were CD62L<sup>hi</sup>. Interestingly, the majority of the TILs from the 9-28- $\zeta$ -CAR-Ts treated mice shifted towards the CD62L low (lo) phenotype, which is typical for TEM cells (Figure 5B). There was no difference in the phenotype of the T cells from the spleens of the mice treated with any of the three T cell therapies, which had similar percentages of the CD62L<sup>hi</sup> population (data not shown). To investigate whether 9-28- $\zeta$ -CAR-Ts not only accumulated at the tumor site but also proliferated there, we isolated CD8<sup>+</sup> cells from the tumors (Figure 5C) and measured the expression of the Ki-67 proliferation marker. Indeed, compared to mock and 9- $\zeta$ -CAR-Ts, only 9-28- $\zeta$ -CAR-Ts proliferated at the tumor site. This Ki-67

positive population was present in the G2/M phases of the cell cycle, as determined by the PI staining for DNA content (Figure 5C).

### **CAR-mediated rejection depends on IFN $\gamma$ R expression on the tumor stroma**

By analyzing the tumors for the cancer cells and stroma cells content, we found that large established SKOV3 tumors contained ~15% of HER-2<sup>+</sup> cancer cells while the other 85% were stroma cells (Supplementary Fig. S5A). The majority of the stroma cells in the SKOV3 tumors were of non-hematopoietic origin (>90% CD45.2 negative, Supplementary Fig. S5A). To investigate whether CAR-mediated tumor rejection requires targeting of the tumor stroma by IFN $\gamma$ , we treated Rag<sup>-/-</sup> and IFN $\gamma$ R<sup>-/-</sup>/Rag<sup>-/-</sup> mice bearing ~3 weeks old SKOV3 tumors (6.6 mm; SD  $\pm$  1.5 mm) with mock or 9-28- $\zeta$ -CAR-Ts. In Rag<sup>-/-</sup> mice, tumors were again rejected following treatment with 9-28- $\zeta$ -CAR-Ts (Figure 6A and Table 1). However, following treatment with 9-28- $\zeta$ -CAR-Ts, tumors progressed in IFN $\gamma$ R<sup>-/-</sup>/Rag<sup>-/-</sup> mice at a comparable kinetic to that seen in mock-treated mice (Figure 6A and Table 1).

In the current settings, IFN $\gamma$  secreted by the transferred T cells could have contributed to tumor eradication either by direct stroma destruction (10,31) or indirectly by activating NK cells and M1 macrophages (21,25). To answer this question, we compared the NK cells and macrophages infiltration in the tumors of mock, 9- $\zeta$ -CAR-T and 9-28- $\zeta$ -CAR-T treated tumor-bearing mice. Tumors from the mice that received 9-28- $\zeta$ -CAR-Ts had a high percentage of infiltrating NK cells (30%) compared to tumors from 9- $\zeta$ -CAR-T (10%) and mock (4%) treated mice (Figure 6B). Tumors isolated from 9- $\zeta$ -CAR-T treated mice contained about 2x more NK cells than tumors from mock treated mice (Figure 6B), which is not surprising since we showed that 9- $\zeta$ -CAR-Ts secrete IFN $\gamma$  upon antigen recognition. The numbers of tumor infiltrating macrophages (F4/80/CD11b double positive) did not vary much between 9-28- $\zeta$ -, 9- $\zeta$ -CAR-T and mock treated mice (Figure 6C).

Nevertheless, macrophages in tumors from 9-28- $\zeta$ -CAR-T treated mice had a marked increase in MHC class II expression (80%) which is typical for M1 macrophage population, while the percentages were much lower for 9- $\zeta$ -CAR-T (43%) and mock (28%) treated mice (Figure 6C). These findings indicate that the IFN $\gamma$  secreted by 9-28- $\zeta$ -CAR-Ts activated NK cells and M1 macrophages. To investigate the role of NK cell activation in tumor rejection, we performed an *in vivo* NK cell depleting experiment. Tumor bearing mice received a-NK 1.1 antibody or isotype (iso) control weekly over the period of 85 days (starting two days before ATT) which depleted the NK cells in the blood (Supplementary Fig. S5B). Mock treated mice did not receive any additional treatment and tumors progressed (Figure 6D). Mice that were treated with a-NK 1.1 antibody and isotype control received 9-28- $\zeta$ -CAR-Ts, and during the observation time of 82 days post ATT majority of the tumors were rejected for both groups (2/3 for isotype control and 4/5 for NK depleted) (Figure 6D). This indicates that NK cells were not necessary for the CAR-mediated tumor rejection.

## **Discussion**

Our study showed for the first time that CAR-Ts were able to reject large solid tumors exclusively by CAR-mediated CD8<sup>+</sup> T cell effector function and independent of CD4<sup>+</sup> T cell or B cell contribution. Costimulation provided by the CD28 signaling domain of the 9-28- $\zeta$ -CAR was essential for tumor rejection in our model and could not be compensated for by increasing the affinity of the scFv domain of the  $\zeta$ -CARs. The inability of  $\zeta$ -CAR-Ts to secrete IL-2 may have contributed to their failure to proliferate, differentiate into TEM and accumulate at the tumor site to mediate HER-2-specific tumor rejection. Another reason for therapy failure might have been the tumor burden; perhaps  $\zeta$ -CAR-Ts would have been more effective against smaller tumors (26).

Both antigen-dependent and -independent mechanisms can contribute to stroma destruction as a requirement for cancer eradication (27). Previous studies of TCR-mediated ATT consistently reported that tumor stroma targeting was critical to prevent tumor recurrence and that T cell-produced IFN $\gamma$  needed to act on the tumor stroma (8,11). However, likely due to the use of different experimental models, different mechanisms were suggested to explain this. When using a surrogate antigen expressed at a high level, antigen cross-presentation by stroma cells was essential for bystander elimination of antigen loss variants (7,8), while targeting a CDA (like SV40 large T antigen) did not require antigen cross-presentation for tumor eradication in a H-2 mismatched host (10,11). Excluding that cross-dressing by the peptide-MHC (28) could have contributed to stroma recognition in the H-2 mismatched host, it appeared but was not formally proven that antigen recognition only on the cancer cells was sufficient for tumor rejection. This could have resulted from the induction of IFN $\gamma$  production by the T cells, which then acted on stroma cells in an antigen-independent fashion either by direct stroma destruction or indirectly by activating the non T cell immune compartment (10,11,29,30). We proved the initial assumption in our current study because CAR-Ts recognized HER-2 exclusively on the cancer cells but not tumor stroma, yet IFN $\gamma$  responsiveness by the stroma was essential for tumor rejection. There was a correlation between increase in the M1 macrophage numbers and tumor rejection in our model, however, it is not clear whether the macrophages directly contributed to tumor rejection, or whether simply the increase was due to higher number of T cells secreting IFN $\gamma$  in the tumors. Similarly, IFN $\gamma$  led to NK cell activation, but despite the increased numbers of NK cell infiltrates in tumors of 28- $\zeta$ -CAR-T treated mice, the CAR-mediated tumor rejection was not dependent on NK cells. In accordance with our previous studies (10,31), it is possible that the mechanism of IFN $\gamma$  acting on tumor stroma has a direct effect involving destruction of tumor vasculature. However, we cannot completely exclude that direct targeting of some stroma cells may have been mediated by recognition of

acquired tumor-derived microvesicles containing HER-2, since such acquisition was observed for some surface receptors (32).

Due to species-specific binding, the IFN $\gamma$  secreted by the mouse T cells could only act on the tumor stroma but not on the cancer cells, which might explain the prolonged rejection time required in our model. Simultaneous cancer and stroma cell targeting would have probably accelerated tumor rejection, as is the case in other models where both tumor compartments were targeted by IFN $\gamma$  (7,9,10). Furthermore, the inability of 9-28- $\zeta$ -CAR-Ts therapy to induce initial tumor regression in IFN $\gamma$ R<sup>-/-</sup>/Rag<sup>-/-</sup> mice could be attributed to this specific setting, in which both cancer and stroma cells were not responsive to IFN $\gamma$  (11).

Although targeting stroma cells by IFN $\gamma$  was essential for tumor rejection in our model, we cannot exclude that stroma cell targeting would have been dispensable in a setting where also cancer cells responded to IFN $\gamma$ . However, in the cases when human CAR-Ts were used for therapy and cancer cells responded to IFN $\gamma$ , established tumors could not be completely rejected (3,17), further implying at the relevance of IFN $\gamma$ -stroma cell targeting for tumor rejection. Therefore, it will be important in future studies to elucidate the relative contribution of antigen-dependent (7,8) and -independent (10,11) destruction of tumor stroma and whether our data are related to targeting a CDA.

Despite the effectiveness of tumor rejection by 9-28- $\zeta$ -CAR, we do not suggest using HER-2-CARs in the clinic, because we did not address potential toxicity in regard to HER-2 expression on normal cells. However, our data are clinically relevant because tumor-specific antigens accessible for CARs have been described (15,16) and will be evaluated for clinical use (33). Taken together, our results show that antigen-independent tumor stroma destruction is required for CAR-mediated cancer eradication.

### **Acknowledgments**

The authors thank M. Hensel and S. Kupsch for technical assistance, and Rosa Karlič for the statistical analysis.

### **Authors' Contributions**

J.C., T.B., A.T. and J.L. designed research; A.T., J.L., L.W., C.P., A.K. and J.C. performed research; M.C. and H.A. provided reagents; A.T., J.L., L.W., J.C. and T.B. analyzed data; A.T., H.A., T. B. and J.C. wrote the manuscript.

### **Grant Support**

This work was supported by the Deutsche Krebshilfe (J.C. and T. B.) and by Deutsche Forschungsgemeinschaft Transregio-Sonderforschungsbereich TR36 (J. C. and T. B.).

## References

1. Eshhar Z, Waks T, Gross G, Schindler DG. Specific activation and targeting of cytotoxic lymphocytes through chimeric single chains consisting of antibody-binding domains and the gamma or zeta subunits of the immunoglobulin and T-cell receptors. *Proc Natl Acad Sci U S A* 1993;90:720–4.
2. Kershaw MH, Westwood JA, Parker LL, Wang G, Eshhar Z, Mavroukakis SA, et al. A phase I study on adoptive immunotherapy using gene-modified T cells for ovarian cancer. *Clin Cancer Res* 2006;12:6106–15.
3. Carpenito C, Milone MC, Hassan R, Simonet JC, Lakhai M, Suhoski MM, et al. Control of large, established tumor xenografts with genetically retargeted human T cells containing CD28 and CD137 domains. *Proc Natl Acad Sci U S A* 2009;106:3360–65.
4. Kochenderfer JN, Wilson WH, Janik JE, Dudley ME, Stetler-Stevenson M, Feldman SA, et al. Eradication of B-lineage cells and regression of lymphoma in a patient treated with autologous T cells genetically engineered to recognize CD19. *Blood* 2010;116:4099–102.
5. Porter DL, Levine BL, Kalos M, Bagg A, June CH. Chimeric antigen receptor-modified T cells in chronic lymphoid leukemia. *N Engl J Med* 2011;365:725–33.
6. Yu P, Rowley DA, Fu Y-X, Schreiber H. The role of stroma in immune recognition and destruction of well-established solid tumors. *Curr Opin Immunol* 2006;18:226–31.
7. Spotto MT, Rowley DA, Schreiber H. Bystander elimination of antigen loss variants in established tumors. *Nat Med* 2004;10:294–98.

8. Zhang B, Karrison T, Rowley DA, Schreiber H. IFN-gamma- and TNF-dependent bystander eradication of antigen-loss variants in established mouse cancers. *J Clin Invest* 2008;118:1398–404.
9. Charo J, Perez C, Buschow C, Jukica A, Czeh M, Blankenstein T. Visualizing the dynamic of adoptively transferred T cells during the rejection of large established tumors. *Eur J Immunol* 2011;41:3187–97.
10. Anders K, Buschow C, Herrmann A, Milojkovic A, Loddenkemper C, Kammertoens T, et al. Oncogene-targeting T cells reject large tumors while oncogene inactivation selects escape variants in mouse models of cancer. *Cancer Cell* 2011;20:755–67.
11. Listopad JJ, Kammertoens T, Anders K, Silkenstedt B, Willimsky G, Schmidt K, et al. Fas expression by tumor stroma is required for cancer eradication. *Proc Natl Acad Sci U S A* 2013;110:2276–81.
12. Restifo NP, Marincola FM, Kawakami Y, Taubenberger J, Yannelli JR, Rosenberg SA. Loss of functional beta 2-microglobulin in metastatic melanomas from five patients receiving immunotherapy. *J Natl Cancer Inst* 1996;88:100–108.
13. Choudhury A, Charo J, Parapuram SK, Hunt RC, Hunt DM, Seliger B, et al. Small interfering RNA (siRNA) inhibits the expression of the Her2/neu gene, upregulates HLA class I and induces apoptosis of Her2/neu positive tumor cell lines. *Int J Cancer* 2004;108:71–77.
14. Felsher DW. Tumor dormancy and oncogene addiction. *APMIS*. 2008;116:629–37.
15. Morgan RA, Johnson LA, Davis JL, Zheng Z, Woolard KD, Reap EA, et al.

Recognition of glioma stem cells by genetically modified T cells targeting EGFRvIII and development of adoptive cell therapy for glioma. *Hum Gene Ther* 2012;23:1043–53.

16. Schietinger A, Philip M, Yoshida BA, Azadi P, Liu H, Meredith SC, et al. A mutant chaperone converts a wild-type protein into a tumor-specific antigen. *Science* 2006;314:304–308.
17. Song D-G, Ye Q, Carpenito C, Poussin M, Wang L-P, Ji C, et al. In vivo persistence, tumor localization, and antitumor activity of CAR-engineered T cells is enhanced by costimulatory signaling through CD137 (4-1BB). *Cancer Res* 2011;71:4617–27.
18. Hemmi S, Merlin G, Aguet M. Functional characterization of a hybrid human-mouse interferon gamma receptor: evidence for species-specific interaction of the extracellular receptor domain with a putative signal transducer. *Proc Natl Acad Sci U S A* 1992;89:2737–41.
19. Chmielewski M, Hombach AA, Abken H. CD28 cosignalling does not affect the activation threshold in a chimeric antigen receptor-redirected T-cell attack. *Gene Ther* 2011;18:62–72.
20. Chmielewski M, Hombach A, Heuser C, Adams GP, Abken H. T cell activation by antibody-like immunoreceptors: increase in affinity of the single-chain fragment domain above threshold does not increase T cell activation against antigen-positive target cells but decreases selectivity. *J Immunol* 2004;173:7647-53.
21. Kruschinski A, Moosmann A, Poschke I, Norell H, Chmielewski M, Seliger B, et al. Engineering antigen-specific primary human NK cells against HER-2 positive carcinomas. *Proc Natl Acad Sci U S A* 2008;105:17481–86.

22. Hombach A, Wiczarkowicz A, Marquardt T, Heuser C, Usai L, Pohl C, et al. Tumor-specific T cell activation by recombinant immunoreceptors: CD3 zeta signaling and CD28 costimulation are simultaneously required for efficient IL-2 secretion and can be integrated into one combined CD28/CD3 zeta signaling receptor molecule. *J Immunol* 2001;167:6123–31.
23. Stephan MT, Moon JJ, Um SH, Bershteyn A, Irvine DJ. Therapeutic cell engineering with surface-conjugated synthetic nanoparticles. *Nat Med* 2010;16:1035–41.
24. Engels B, Engelhard VH, Sidney J, Sette A, Binder DC, Liu RB, et al. Relapse or Eradication of Cancer Is Predicted by Peptide-Major Histocompatibility Complex Affinity. *Cancer Cell* 2013;23:516–26.
25. Klug F, Prakash H, Huber PE, Seibel T, Bender N, Halama N, et al. Low-Dose Irradiation Programs Macrophage Differentiation to an iNOS. *Cancer Cell* 2013;24:589–602.
26. Pinthus JH, Waks T, Malina V, Kaufman-Francis K, Harmelin A, Aizenberg I, et al. Adoptive immunotherapy of prostate cancer bone lesions using redirected effector lymphocytes. *J Clin Invest* 2004;114:1774–81.
27. Anders K, Blankenstein T. Molecular pathways: comparing the effects of drugs and T cells to effectively target oncogenes. *Clin Cancer Res* 2013;19:320–26.
28. Dolan BP, Gibbs KD, Ostrand-Rosenberg S. Tumor-specific CD4<sup>+</sup> T cells are activated by “cross-dressed” dendritic cells presenting peptide-MHC class II complexes acquired from cell-based cancer vaccines. *J Immunol* 2006;176:1447–55.
29. Schüler T, Blankenstein T. Cutting edge: CD8<sup>+</sup> effector T cells reject tumors

- by direct antigen recognition but indirect action on host cells. *J Immunol* 2003;170:4427–31.
30. Blankenstein T. The role of tumor stroma in the interaction between tumor and immune system. *Curr Opin Immunol* 2005;17:180–86.
  31. Briesemeister D, Sommermeyer D, Loddenkemper C, Loew R, Uckert W, Blankenstein T, et al. Tumor rejection by local interferon gamma induction in established tumors is associated with blood vessel destruction and necrosis. *Int J Cancer* 2011;128:371–78.
  32. Pucci F, Pittet MJ. Molecular pathways: tumor-derived microvesicles and their interactions with immune cells in vivo. *Clin Cancer Res* 2013;19:2598–604.
  33. Riddell SR, Jensen MC, June CH. Chimeric Antigen Receptor–Modified T Cells: Clinical Translation in Stem Cell Transplantation and Beyond. *Biol Blood Marrow Transplant* 2013;19:S2–S5.

### **Figure Legends**

**Figure 1.** Mouse T cells express the HER-2-specific CARs and secrete IFN $\gamma$  when stimulated with SKOV3 target cells, but only recognition by 9-28- $\zeta$ -CAR leads to production of IL-2. A, HER-2-specific  $\zeta$ -CAR constructs of five different affinities (KD:  $3.2 \times 10^{-7}$ – $1.5 \times 10^{-11}$  M) and HER-2-specific 28- $\zeta$ -CAR construct of intermediate affinity

(KD;  $1 \times 10^{-9}$ ) were cloned into pMSCV vector. The resulting retroviral vectors were designated as pMSCV-7- $\zeta$ -CAR for the lowest affinity (KD:  $3.2 \times 10^{-7}$  M), pMSCV-8- $\zeta$ -CAR for the wild type construct (KD:  $1.6 \times 10^{-8}$  M), followed by pMSCV-9- $\zeta$ -, pMSCV-10- $\zeta$ - and pMSCV-11- $\zeta$ -CAR constructs with the increasing affinities of KD:  $1 \times 10^{-9}$ ,  $1.2 \times 10^{-10}$  and  $1.5 \times 10^{-11}$  M, respectively. pMSCV-9-28- $\zeta$ -CAR is the resulting retroviral vector for the dual signaling CAR with intermediate affinity of KD:  $1 \times 10^{-9}$  M. B, splenocytes derived from ChRLuc/OT-1/Rag<sup>-/-</sup> mice were transduced with different CAR constructs. Untransduced (-) and CAR transduced T cells were stained with  $\alpha$ -CD8 and  $\alpha$ -hlgG Abs and analyzed by flow cytometry. C, splenocytes derived from OT-1/Rag<sup>-/-</sup> mice were transduced with different  $\zeta$ -CARs and with the 9-28- $\zeta$ -CAR. The average expression for  $\zeta$ -CARs was 6% (SD  $\pm$  3%) and 5% for the 9-28- $\zeta$ -CAR. Mock and CAR transduced T cells were cocultured with titrated numbers of SKOV3 cells for 24h and levels of secreted IFN $\gamma$  and IL-2 were measured by ELISA. Data represent mean values of triplicates and one representative experiment of two is shown.

**Figure 2.** Engineering T cells with high affinity  $\zeta$ -CARs does not lead to tumor rejection. Rag<sup>-/-</sup> mice were challenged with  $5 \times 10^6$  SKOV3 cells. Approximately three weeks post tumor inoculation, tumor-bearing mice were treated with  $2 \times 10^6$  ChRLuc/OT-1/Rag<sup>-/-</sup>  $\zeta$ -CAR-Ts or mock T cells. The percentage of CAR expression for 7-, 8-, 9- 10- and 11- $\zeta$ -CAR was 5, 8, 7, 7 and 5%, respectively. Indicated is mean tumor diameter over the time period of the experiment for each mouse (each line), n=2 for mock, n=3 for 7-, 8- 10- and 11- $\zeta$ -CAR, and n=4 for 9- $\zeta$ -CAR. Each line represents a mean tumor diameter in a single mouse. Shown is one representative experiment out of two.

**Figure 3.** CAR-Ts expressing 9-28- $\zeta$ -CAR reject large established SKOV3 tumors in Rag<sup>-/-</sup> mice. A, Rag<sup>-/-</sup> mice bearing three weeks old SKOV3 tumors received  $2 \times 10^6$

CAR-Ts derived from ChRLuc/OT-1/Rag<sup>-/-</sup> expressing expressing CARs of the same affinity but different signaling molecules (9-28-ζ-CAR (n= 3), 9-ζ-CAR (n= 3)) or mock transduced (n= 2). The percentage of CAR<sup>+</sup> T cells was 28% and 7% for 9-28-ζ-CAR and 9-ζ-CAR, respectively. B, depicted are mice (n= 3 for each treatment) from the same experiment as in (A), which were treated with lower numbers of 9-28-ζ-CAR-Ts (2x10<sup>5</sup> or 5x10<sup>4</sup>). In total three experiments were performed for ATT with 2x10<sup>6</sup> T cells, two with 2x10<sup>5</sup> and one with 5x10<sup>4</sup> T cells. C, four weeks post SKOV3 tumor challenge Rag<sup>-/-</sup> mice were treated with 2x10<sup>6</sup> CAR-Ts (ChRLuc/OT-1/Rag<sup>-/-</sup>) expressing 9-ζ-CAR, 9-28-ζ-CAR or mock T cells (n= 2 for each treatment). The percentage of CAR<sup>+</sup> cells was similar for the 9-ζ- and 9-28-ζ-CAR-Ts (10% and 8%, respectively). Each line represents a mean tumor diameter of a single mouse. Data are representative of 2 independently performed experiments.

**Figure 4.** CAR-Ts expressing ζ-CAR fail to expand and to accumulate specifically at the tumor site while 28-ζ CAR-Ts do. A, T cell signal at the tumor site of the adoptively transferred CAR-Ts (derived from ChRLuc/OT-1/Rag<sup>-/-</sup> mice) was followed over time. The shaded box represents the background signal, which was set to 1x10<sup>5</sup> photon/s/cm<sup>2</sup>/steradian. Each line represents the signal emitted at the tumor site from a single mouse (n=2 for mock, n=3 for the all five ζ-CARs, n=4 for the 9-28-ζ-CAR). B, T cell signal for one representative mouse is shown on different indicated days post ATT for mice receiving mock, 9-ζ- or 9-28-ζ-CAR-Ts. C, shown are mice with tumor rejection imaged to detect FLuc signal emitted by the tumor cells. Data are representative of 2 independently performed experiments.

**Figure 5.** 9-28-ζ-CAR-Ts differentiate into effector memory T cells and proliferate at the tumor site. A, splenocytes from ChRLuc/OT-1/Rag<sup>-/-</sup> mice were either left untreated (naïve) or were transduced with mock, 9-ζ-CAR or 9-28-ζ-CAR retroviruses. Two days after last transduction, cells were stained with a-CD3, a-CD44

and a-CD62L antibodies and analyzed by flow cytometry. Shown are CD3 gated cells. B, single tumor cells (day 16 post ATT) were labeled with a-CD8, a-CD44 and a-CD62L antibodies. Shown are CD8/CD44 gated cells of one representative tumor sample per group out of two. C, shown are CD8<sup>+</sup> cells that were MACS sorted with 85% purity from two pooled tumor samples for each treatment (mock, 9- $\zeta$ -CAR or 9-28- $\zeta$ -CAR) and labeled with PI and a-Ki-67 antibody (day 31 post ATT).

**Figure 6.** 9-28- $\zeta$ -CAR-mediated rejection of SKOV3 tumors requires IFN $\gamma$ R expression by the tumor stroma, and is NK cell independent. A, Rag<sup>-/-</sup> and IFN $\gamma$ R<sup>-/-</sup>/Rag<sup>-/-</sup> mice were challenged with SKOV3 cells. Approximately three weeks post tumor challenge, mice received OT-1/Rag<sup>-/-</sup> 9-28- $\zeta$ -CAR-Ts (n=4 for A, B and C) or mock T cells (n=2 for A, B and C). A, indicated are mean tumor diameters over time of individual mice from one representative experiment out of two. B, shown are single tumor cells labeled with a-NK 1.1 and a-CD49b (DX5) Ab gated on the lymphocytes for one representative out of two mice analyzed for mock treated tumors and one out of total four for 9- $\zeta$ -CAR and 9-28- $\zeta$ -CAR treated tumors (combined from days 8 and 16 post ATT). C, single cell suspensions of tumors from mice receiving mock T cells, 9- $\zeta$ -CAR-Ts or 9-28- $\zeta$ -CAR-Ts were labeled with a-F4/80, a-CD11b and a-IA-IE Ab. Data are gated on live cells (top panels). Histograms indicate MHC class II expression on F4/80/CD11b double positive cells. Same numbers of tumor samples per treatment are shown as in B. D, Approximately four weeks post tumor challenge mice received 2x10<sup>6</sup> 9-28- $\zeta$ -CAR-Ts (40% CAR<sup>+</sup>). Two days before ATT mice were treated with either a-NK 1.1 (n=5) or isotype control (iso) (n=3) Ab, which was followed by weekly Ab administration throughout the duration of the experiment. Mock treated mice (n=2) did not receive Ab treatment. Indicated are mean tumor diameters of individual mice over time from a single experiment.

**Tables**

construct	recipient	T cell #	rejection	# of experiments	p value
7-ζ-CAR	Rag <sup>-/-</sup>	2x10 <sup>6</sup>	0/6	2	1
8-ζ-CAR	Rag <sup>-/-</sup>	2x10 <sup>6</sup>	0/6	2	1
9-ζ-CAR	Rag <sup>-/-</sup>	2x10 <sup>6</sup>	0/13	4	1
10-ζ-CAR	Rag <sup>-/-</sup>	2x10 <sup>6</sup>	0/6	2	1
11-ζ-CAR	Rag <sup>-/-</sup>	2x10 <sup>6</sup>	0/6	2	1
mock	Rag <sup>-/-</sup>	2x10 <sup>6</sup>	0/15	6	1
	IFNγR <sup>-/-</sup> /Rag <sup>-/-</sup>	2x10 <sup>6</sup>	0/4	2	1
9-28-ζ-	Rag <sup>-/-</sup>	2x10 <sup>6</sup>	21/21	6	0

CAR		$2 \times 10^5$	7/7	2	0.000006
		$5 \times 10^4$	3/3	1	0.001225
	IFN $\gamma$ R <sup>-/-</sup> /Rag <sup>-/-</sup>	$2 \times 10^6$	0/10	2	1

**Table 1.** Total mice numbers. Indicated are numbers of mice that rejected the tumors from total mice in all experiments from different constructs and conditions. *P* value was calculated in comparison to mock treated group using Fisher's exact test.

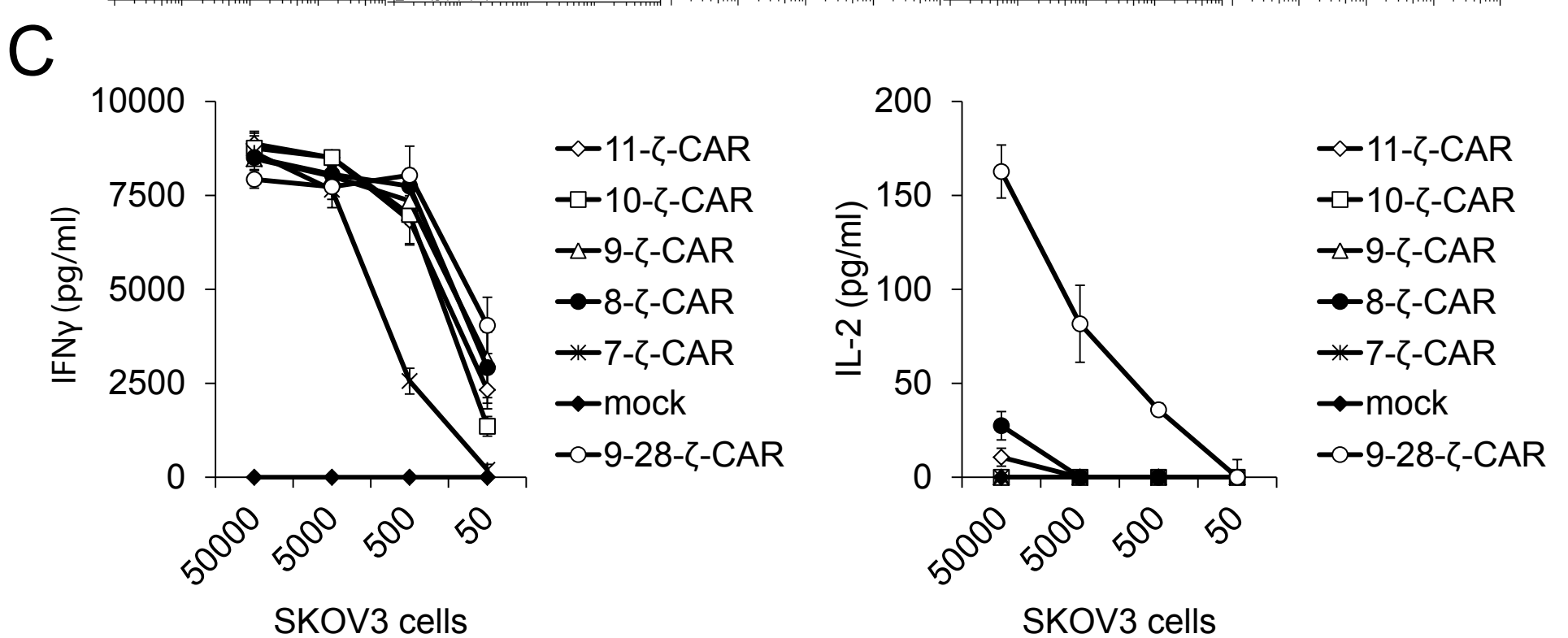
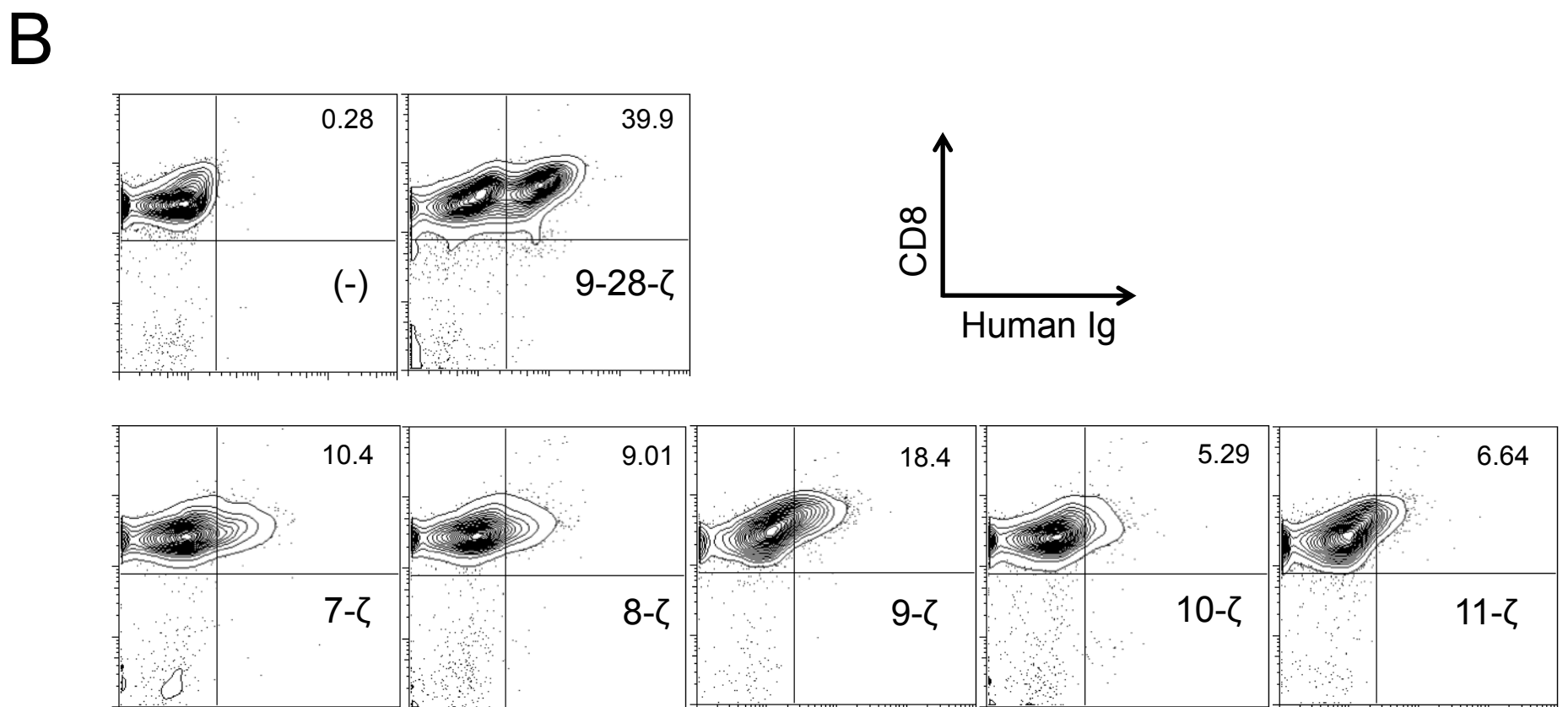
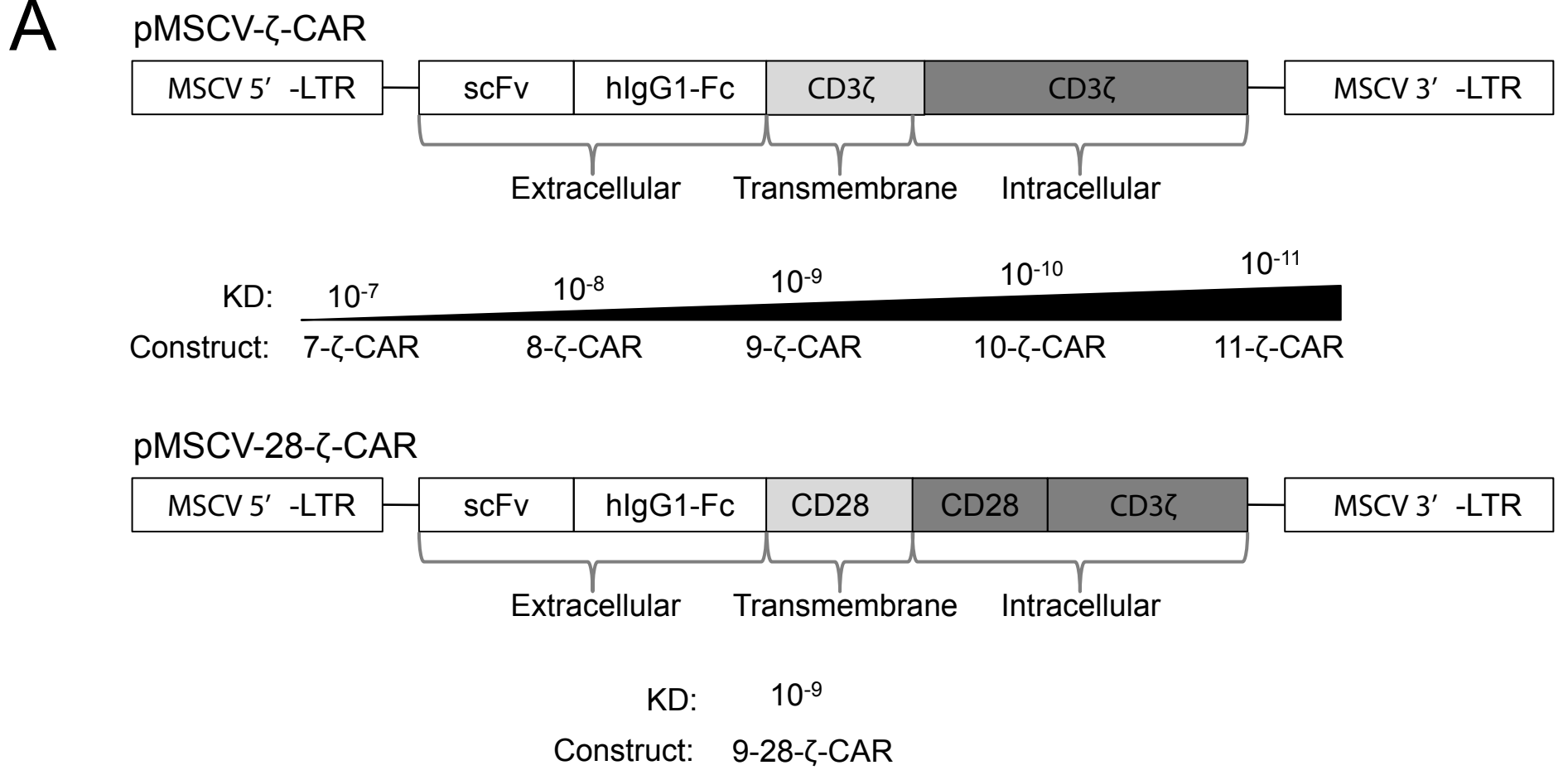


**Figure 1**

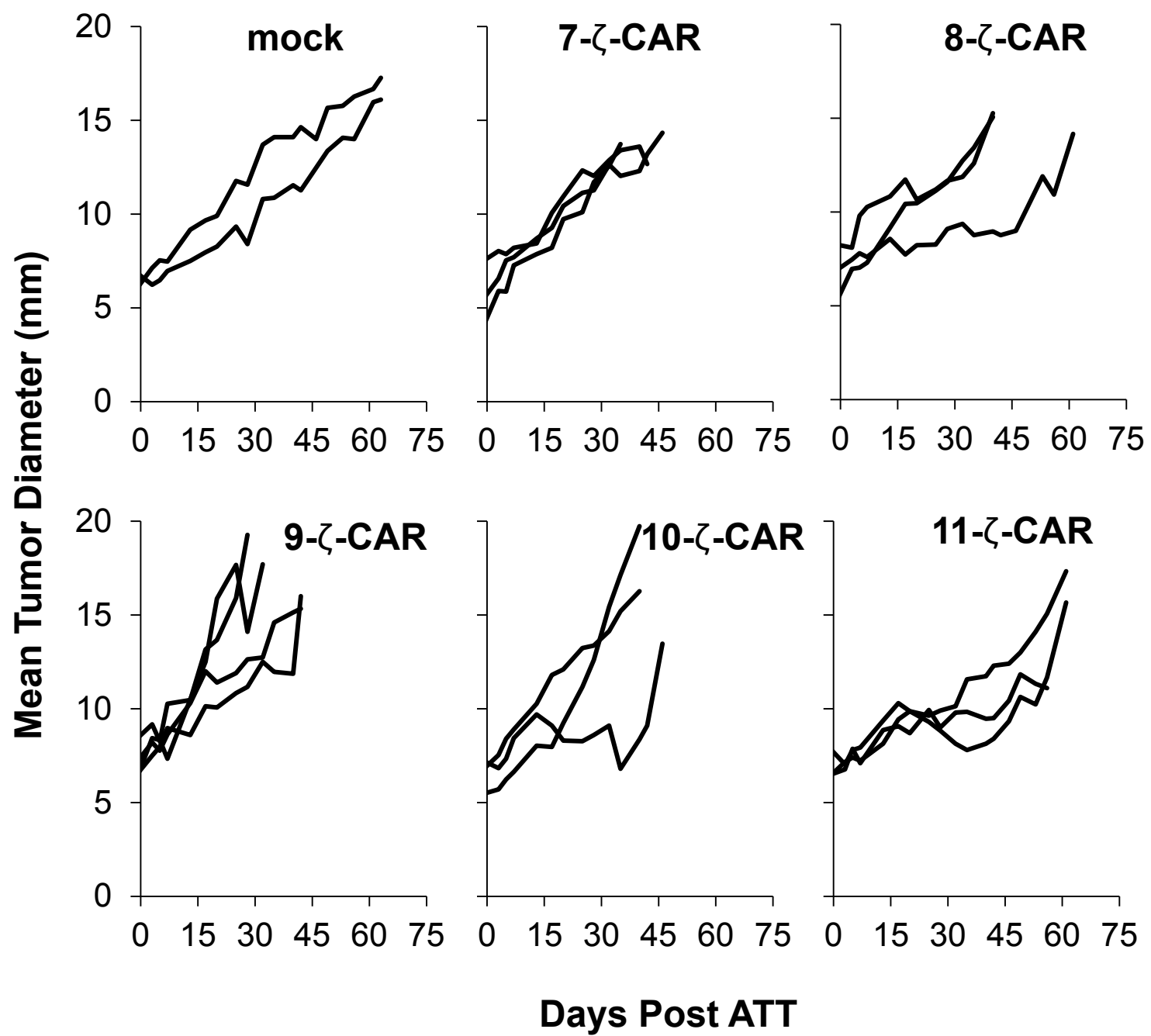


**Figure 2**

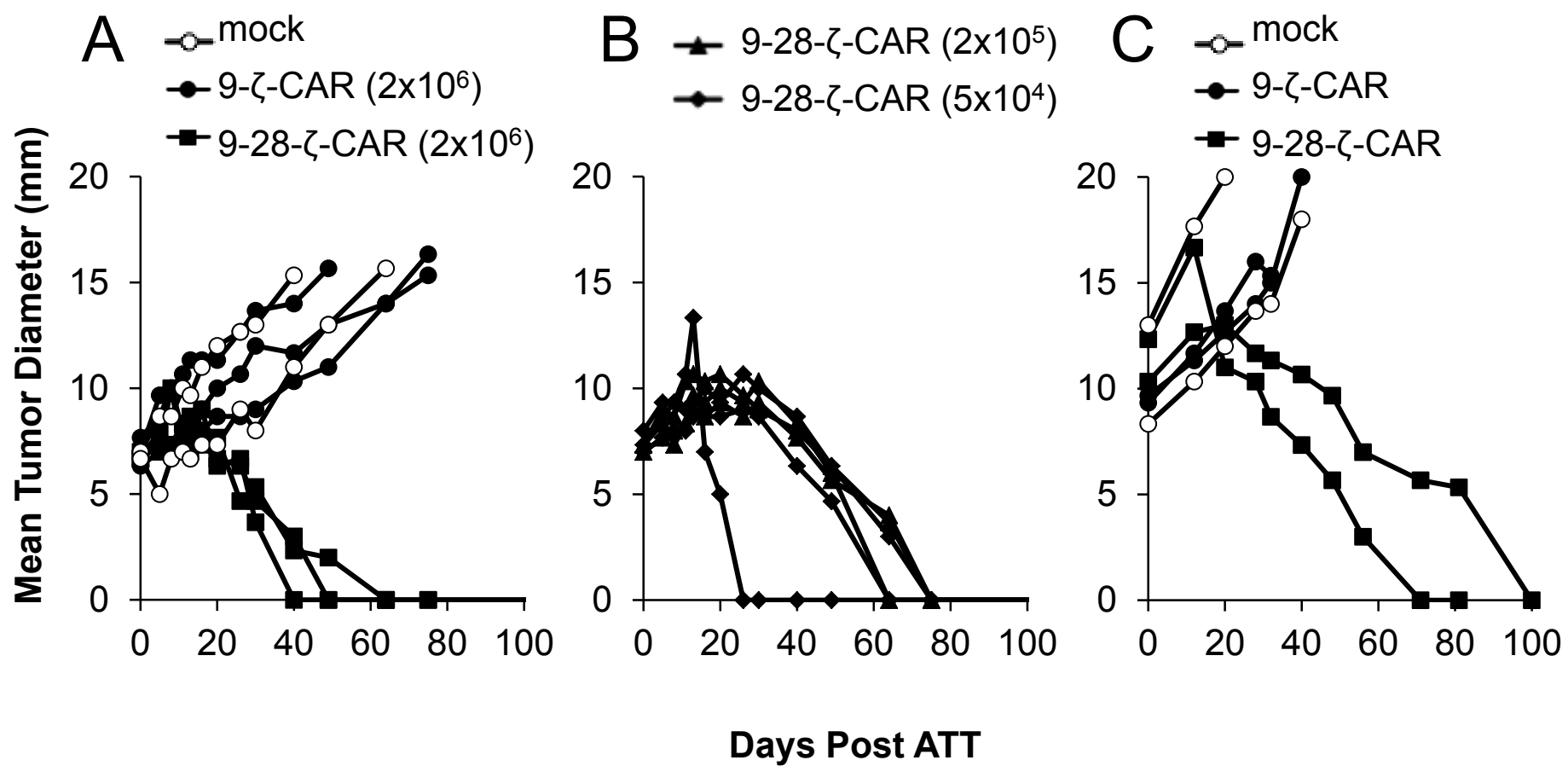


**Figure 3**

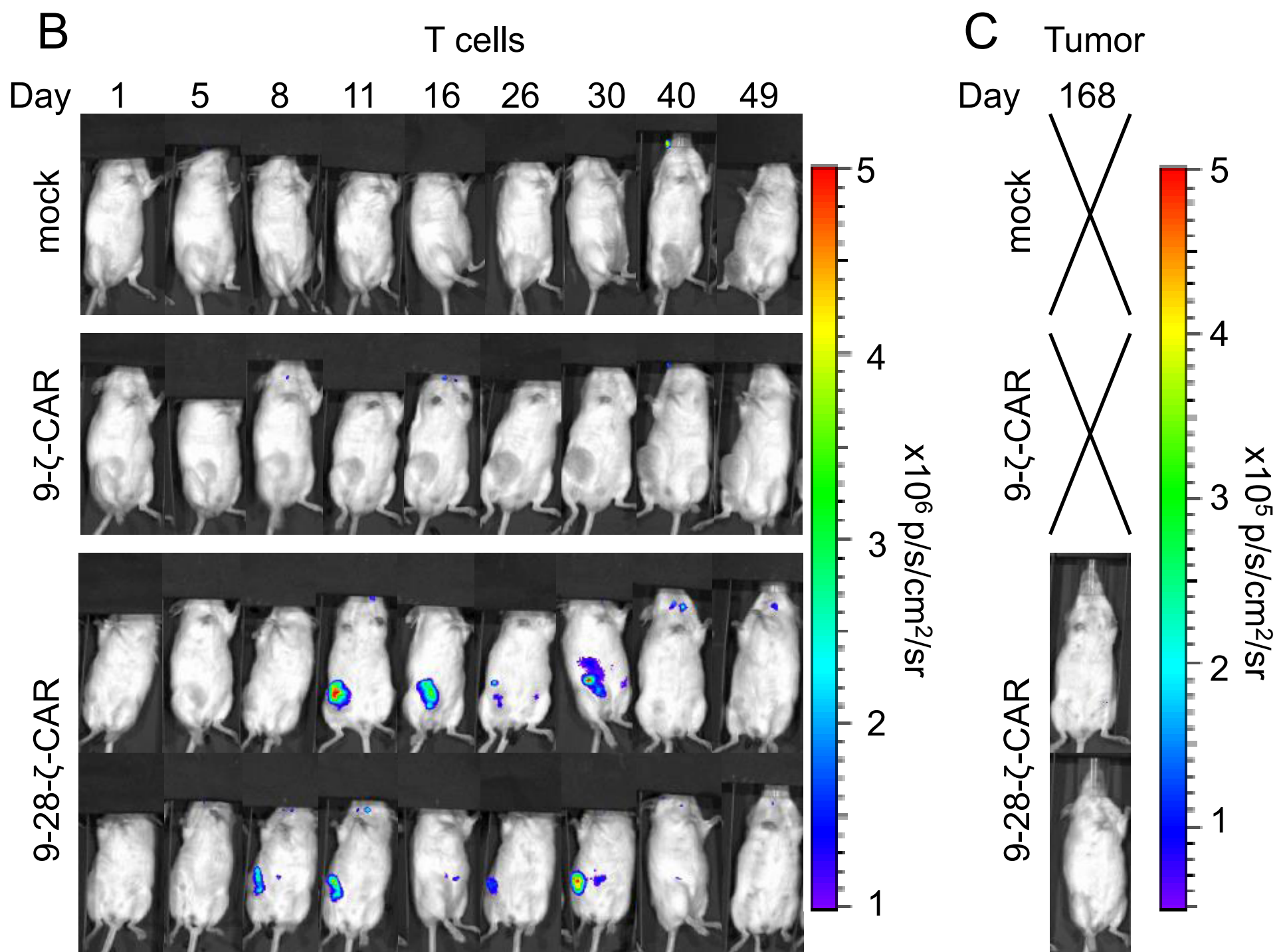
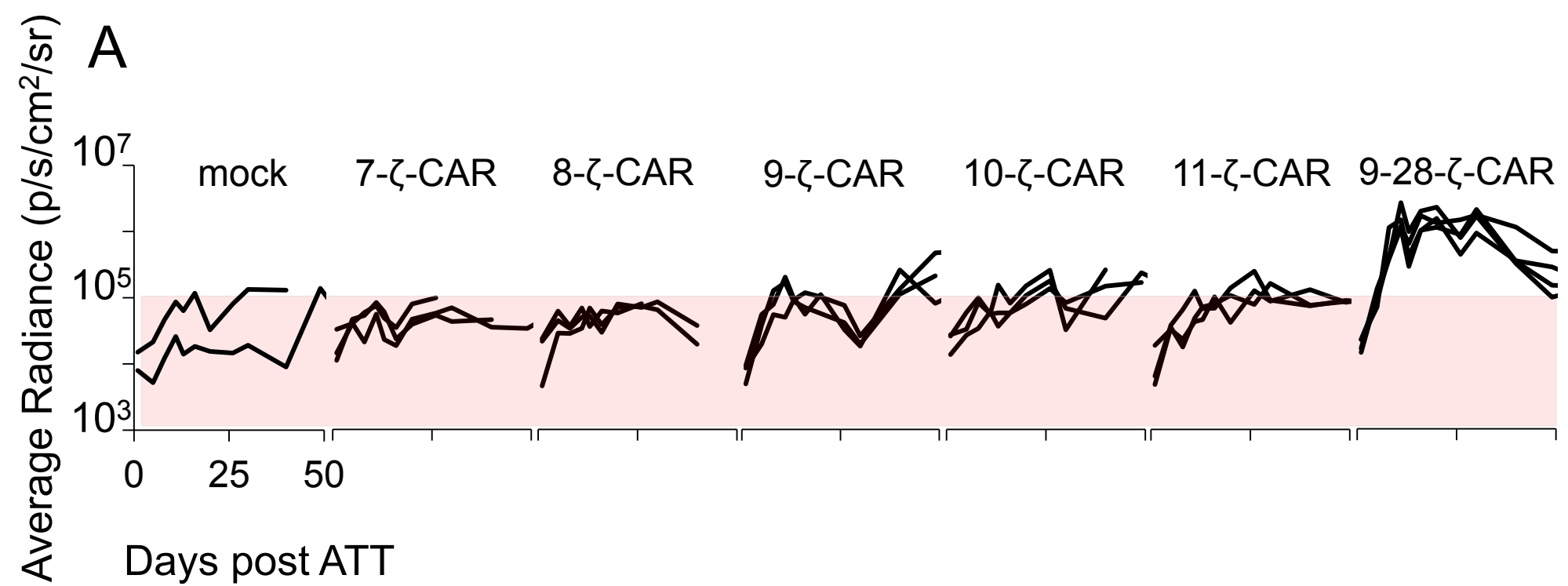


**Figure 4**

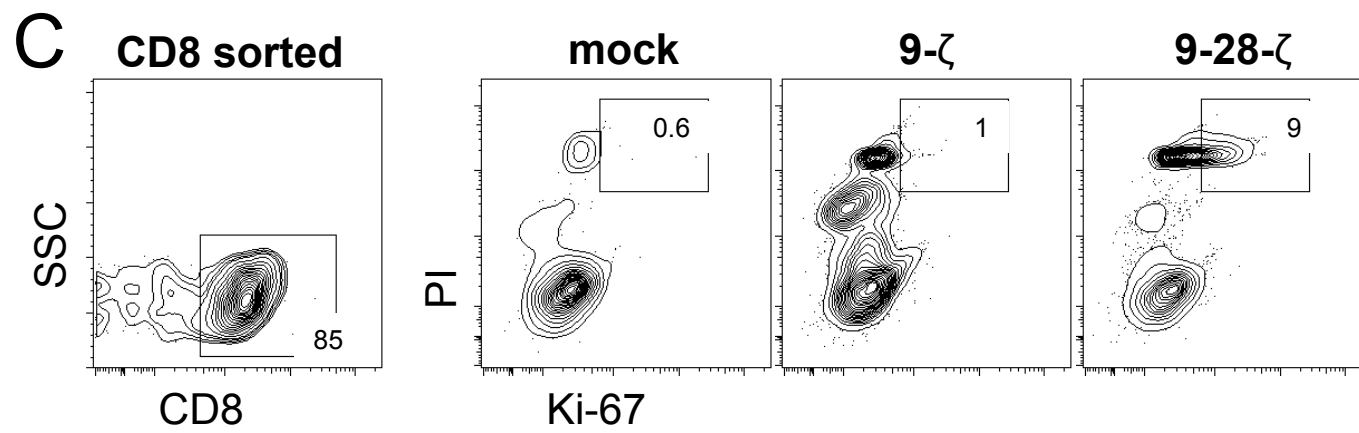
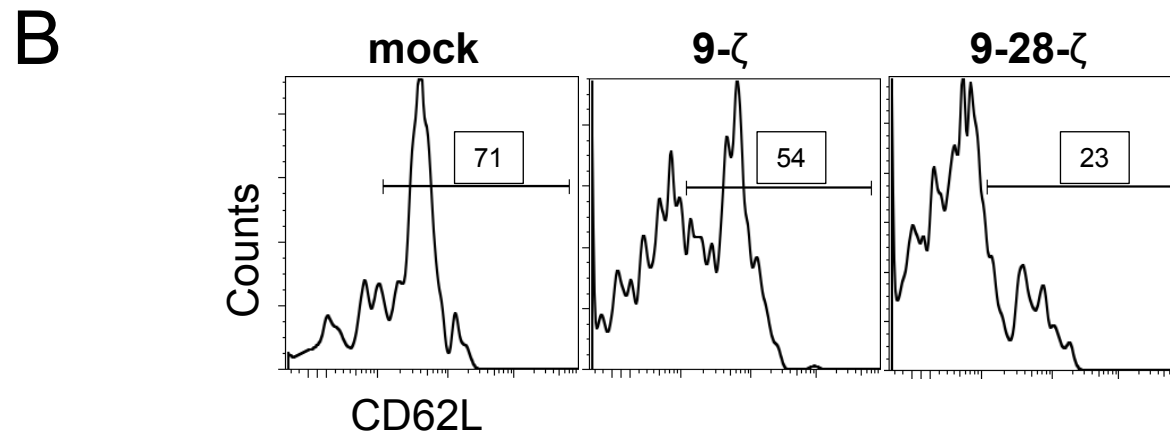
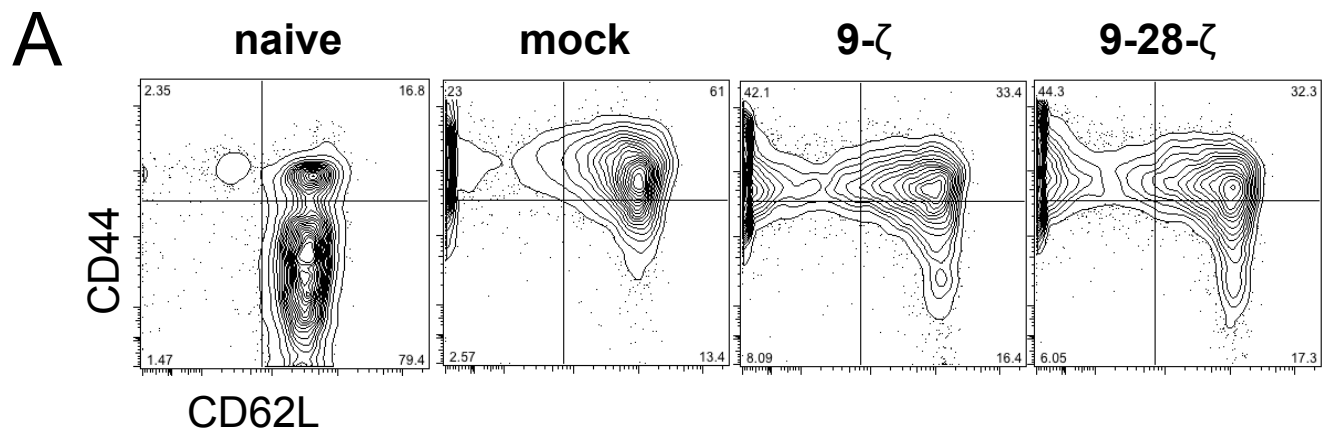


**Figure 5**

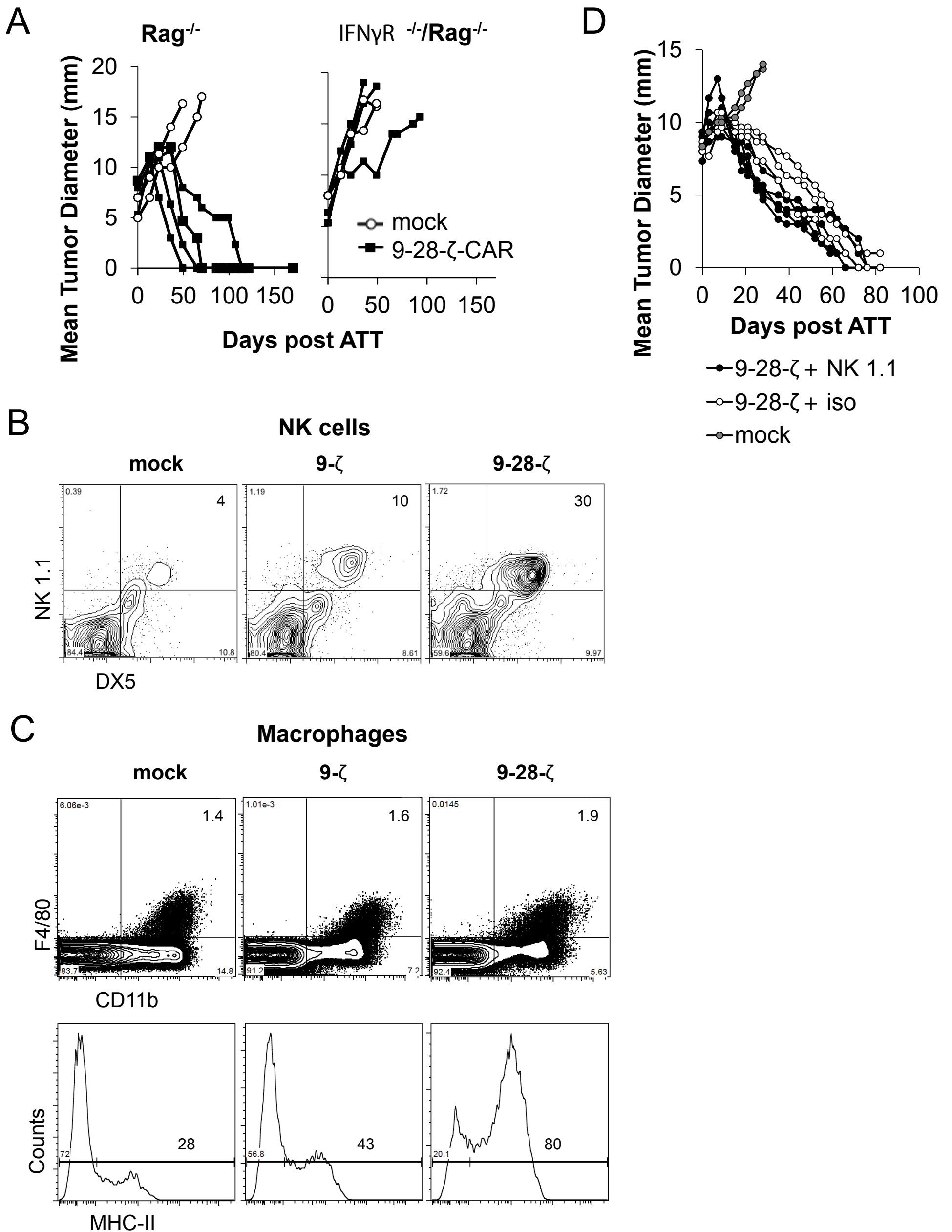


**Figure 6**

## Supplementary Figure Legends

**Supplementary Fig. S1.** Schematic representation of species-specific molecular interactions in models of CAR-mediated tumor rejection. Depicted are T cell effector mechanisms targeting either cancer cells or tumor stroma showing that IFN $\gamma$ /IFN $\gamma$ R interaction is species-specific. The antigen (Ag) is recognized by CAR-Ts directly on the cancer cells but not cross-presented on the tumor stroma. A, previous models utilized human polyclonal T cells as CAR recipients that were allogeneic to the tumor and xenogeneic to the mouse (TCR recognition of mouse and human MHC I). B, our current model surpasses the limitations of the previous models by the use of monoclonal T cells which are syngeneic to the host, and although xenogenic to the tumor there is no TCR recognition of human MHC I because the T cells are OVA-specific.

**Supplementary Fig. S2.** 9-28- $\zeta$ -CAR expression on mouse T cells compared to  $\zeta$ -CARs. The graph shows the percentage of CAR transduced T cells from seven independently performed experiments (all constructs included in each experiment) based on staining with a-hlgG Ab and measured by flow cytometry. The black line indicates the average expression for each of the CAR constructs. *P* value was calculated in comparison to 9-28- $\zeta$ -CAR with one sided t-test ( $*P < 0.05$ , n.s; not significant).

**Supplementary Fig. S3.** Mice treated with  $\zeta$ -CAR-Ts have a slight increase in total body signal when compared to mock treated control mice but less than 9-28- $\zeta$ -CAR-T. Depicted are the same mice from Fig. 4 with the scale set from  $2 \times 10^4$  to  $5 \times 10^6$  photon/s/cm<sup>2</sup>/steradian to visualize the homeostatic expansion of mock T cells, 9- $\zeta$ - and 9-28- $\zeta$ -CAR-Ts.

**Supplementary Fig. S4.** 9-28- $\zeta$ -CAR-Ts accumulate at the tumor site. Mice bearing four weeks old SKOV3 tumors received  $1 \times 10^6$  T cells ( $2 \times 10^5$  CAR<sup>+</sup>) or  $1 \times 10^6$  mock transduced T cells. Shown is one mouse with indicated regions of interest where T cell signal (Total Flux) was measured over time and is shown for each region in a separate chart. Each line indicates the average T cell signals from 4 mock, 7 9- $\zeta$ -CAR-T, and 7 9-28- $\zeta$ -CAR-T treated mice.

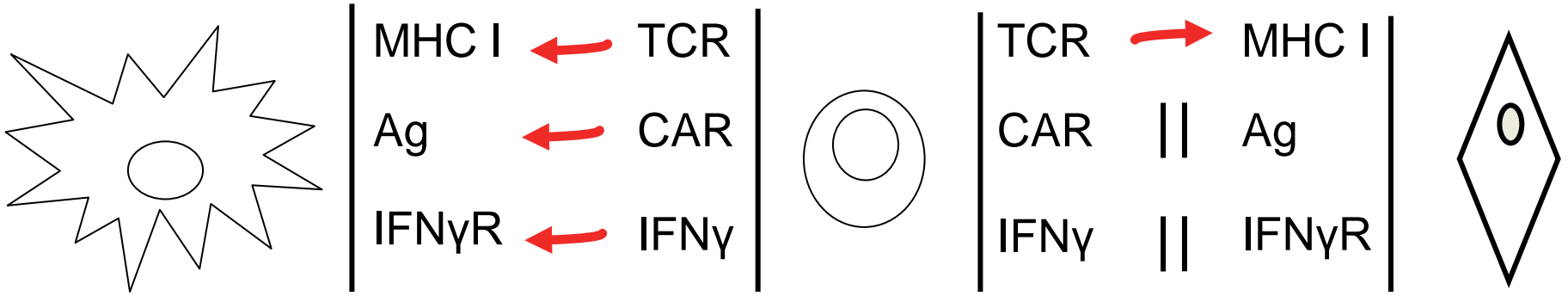
**Supplementary Fig. S5.** Non-hematopoietic cells compose the majority of the SKOV3 tumor stroma. A, shown are live cells from single tumor cell suspension labeled with  $\alpha$ -Her2-Neu and  $\alpha$ -CD45.2. Cells gated on the HER-2 negative population are shown on the right. One representative tumor out of two is shown. B, Depicted is the analysis of NK cell depletion in blood from  $\alpha$ -NK 1.1- or iso-treated mice shown in Figure 6D. Cells were labeled with  $\alpha$ -NK 1.1 and  $\alpha$ -CD49b (DX5) Ab.

**A****Previous models**

Human cancer cells

Human CAR<sup>+</sup> T cells  
(allo/xenogeneic, polyclonal)

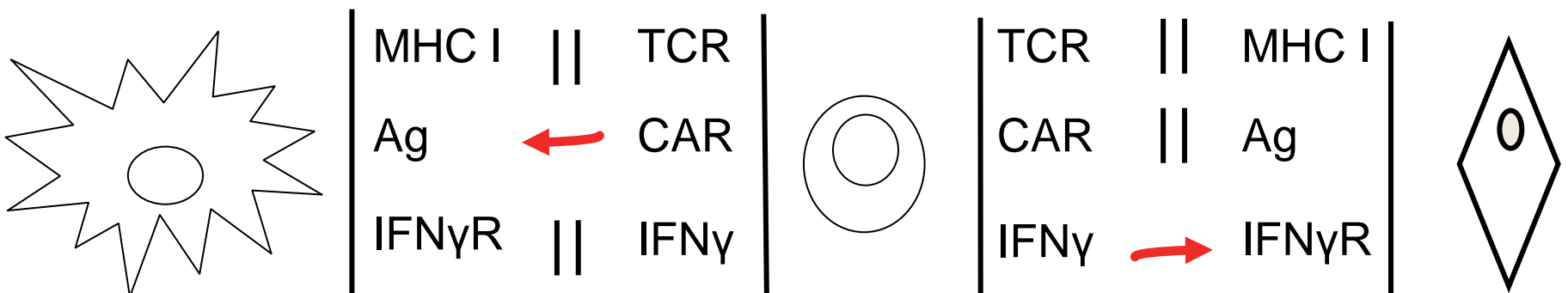
Mouse stroma cells

**B****Current model**

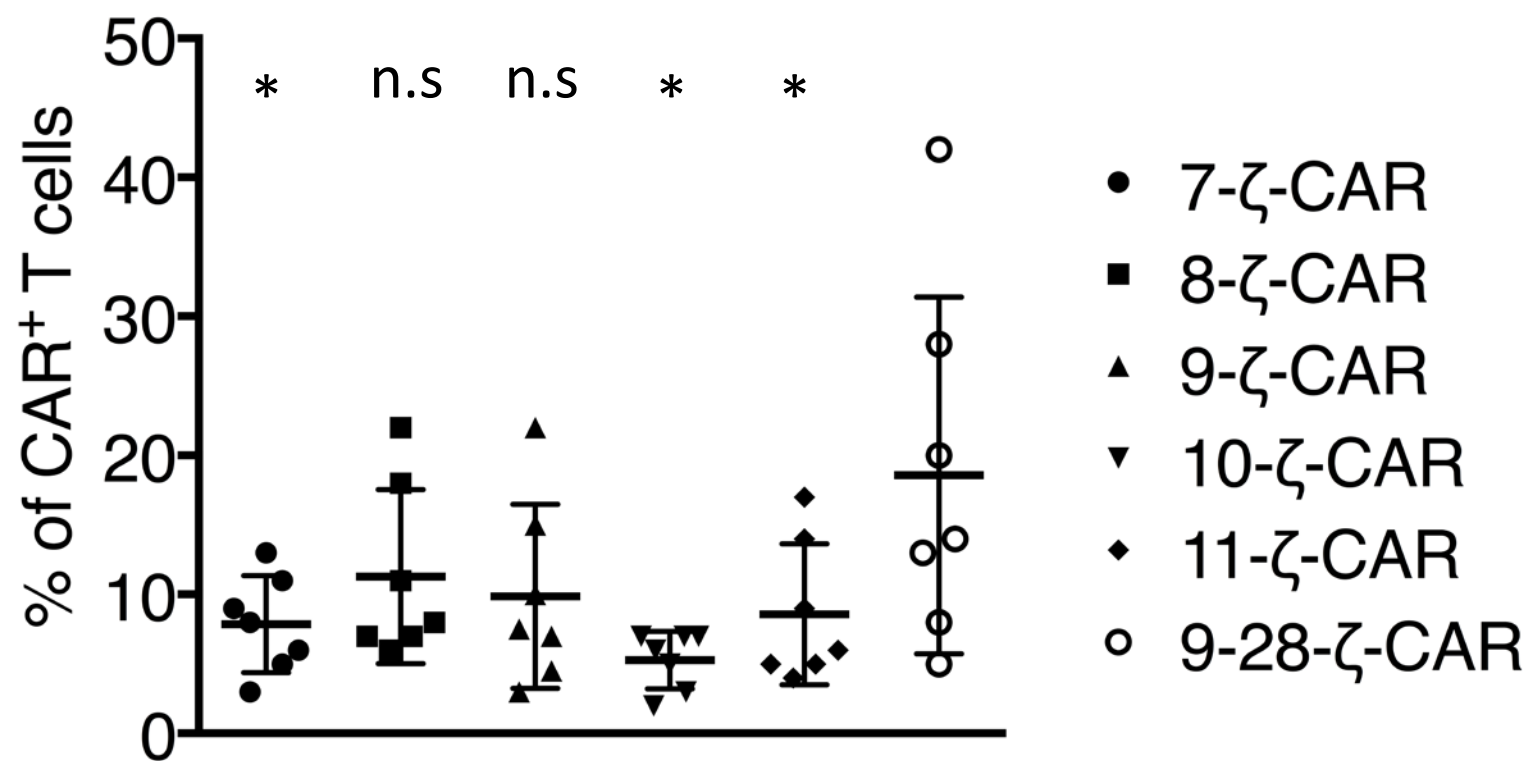
Human cancer cells

Mouse CAR<sup>+</sup> T cells  
(non-specific, monoclonal)

Mouse stroma cells

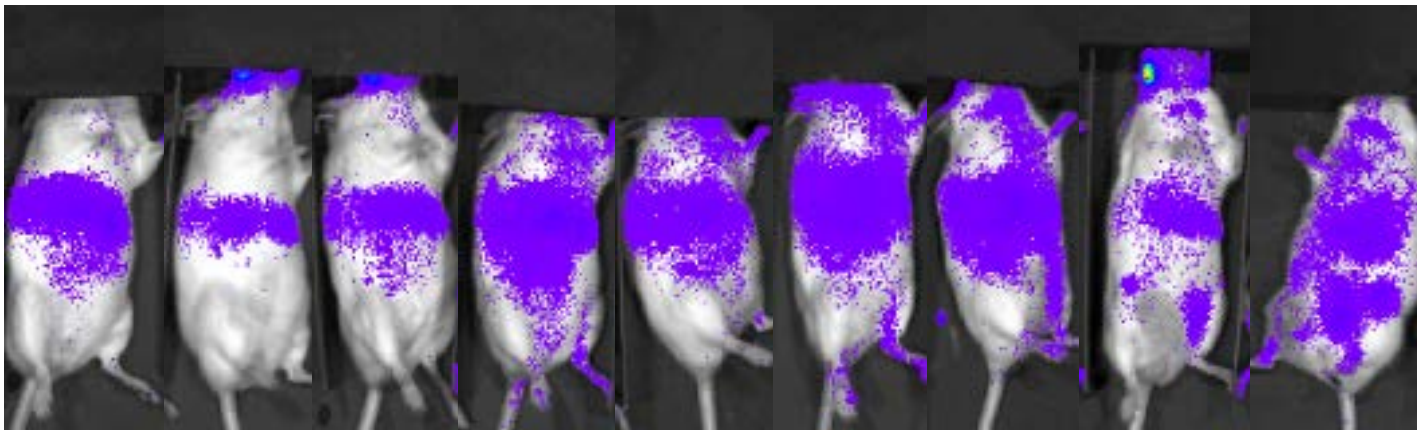


← Interaction      || No interaction

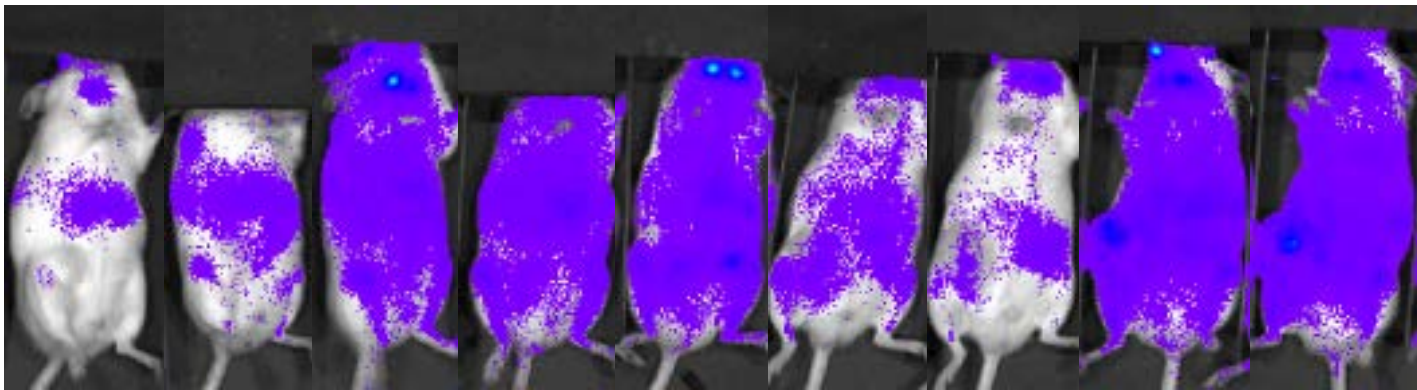


day 1 5 8 11 16 26 30 40 49

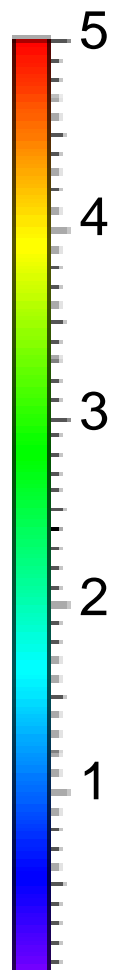
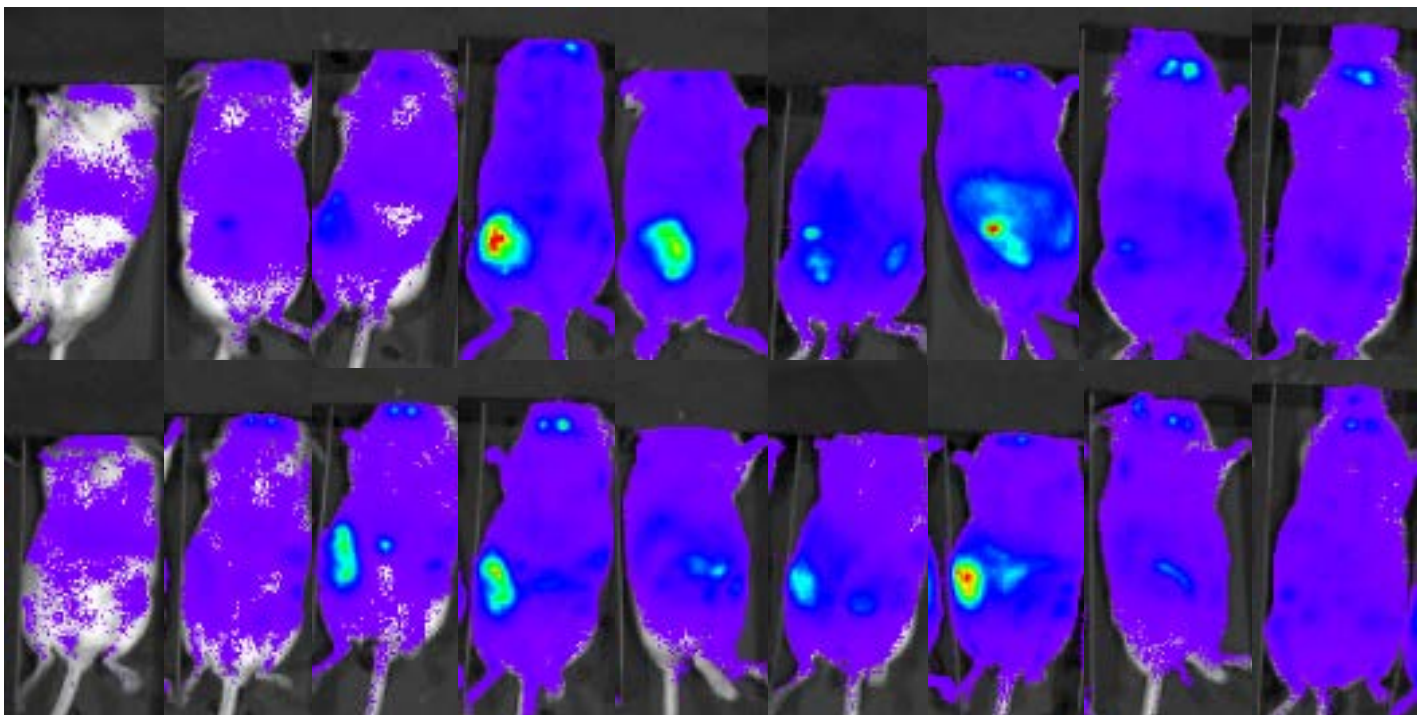
mock



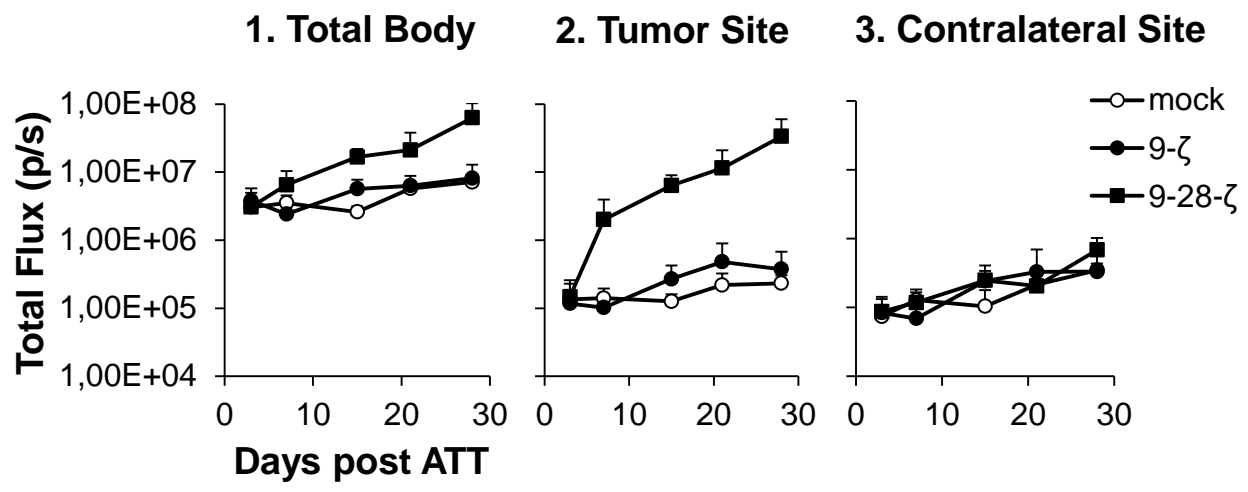
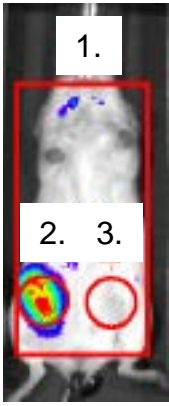
9- $\zeta$ -CAR

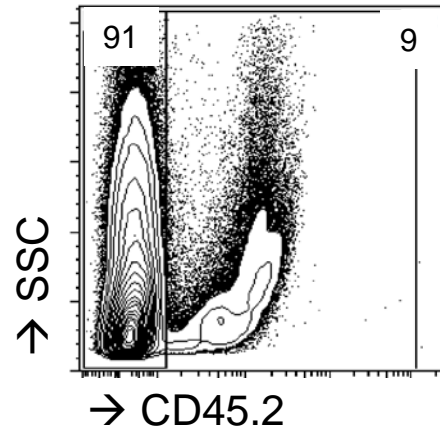
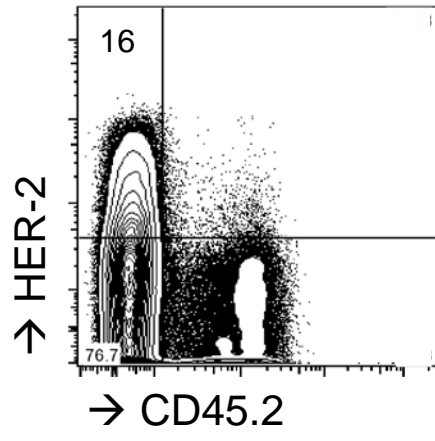


9-28- $\zeta$ -CAR



Min:  $2 \times 10^4$   
Max:  $5 \times 10^6$



**A****B**